NASA TECHNICAL NOTE

NASA TN D-7771

NASA TN D-7771

THE INFLUENCE OF SURFACE WAVES ON WATER CIRCULATION IN A MID-ATLANTIC CONTINENTAL-SHELF REGION

Charles H. Whitlock and Theodore A. Talay

Langley Research Center
Hampton, Va. 23665

NATIONAL AERONAUTICS AND SPACE ADMINISTRATION • WASHINGTON, D. C. • DECEMBER 1974

1. Report No. NASA TN D-7771	2. Government Accession No.	3. Recipient's Catalog No.
4. Title and Subtitle THE INFLUENCE OF SURFACE WAVES ON WATER CIRCULATION IN A MID-ATLANTIC CONTINENTAL-SHELF REGION		5. Report Date December 1974
		6. Performing Organization Code
7. Author(s) Charles H. Whitlock and Theodore A. Talay		8. Performing Organization Report No. L-9699
9. Performing Organization Name and Address NASA Langley Research Center Hampton, Va. 23665		10. Work Unit No. 177-55-35-05
		11. Contract or Grant No.
12. Sponsoring Agency Name and Address National Aeronautics and Space Administration Washington, D.C. 20546		13. Type of Report and Period Covered Technical Note
		14. Sponsoring Agency Code
15. Supplementary Notes		

16. Abstract

The importance of wave-induced currents in different weather conditions and water depths (18.3 m and 36.6 m) is assessed in a mid-Atlantic continental-shelf region. A review of general circulation conditions is conducted. Factors which perturb the general circulation are examined using analytic techniques and limited experimental data. Actual wind and wave statistics for the region are examined. Relative magnitudes of the various currents are compared on a frequency of annual occurrence basis. Results indicate that wave-induced currents are often the same order of magnitude as other currents in the region and become more important at higher wind and wave conditions. Wind-wave and ocean-swell characteristics are among those parameters which must be monitored for the analytical computation of continental-shelf circulation.

17. Key Words (Suggested by Author(s))		18. Distribution Statement	
Ocean circulation Ocean waves Wave-induced currents Oceanography		Unclassified – Unlimited STAR Category 13	
19. Security Classif. (of this report) Unclassified	20. Security Classif. (of this page) Unclassified	21. No. of Pages 45	22. Price* $3.75

*For sale by the National Technical Information Service, Springfield, Virginia 22151

THE INFLUENCE OF SURFACE WAVES ON WATER CIRCULATION IN A MID-ATLANTIC CONTINENTAL-SHELF REGION

By Charles H. Whitlock and Theodore A. Talay
Langley Research Center

SUMMARY

The importance of wave-induced currents in different weather conditions and water depths (18.3 m and 36.6 m) is assessed in a mid-Atlantic continental-shelf region. A review of general circulation conditions is conducted. Factors which perturb the general circulation are examined using analytic techniques and limited experimental data. Actual wind and wave statistics for the region are examined. Relative magnitudes of the various currents are compared on a frequency of annual occurrence basis. Results indicate that wave-induced currents are often the same order of magnitude as other currents in the region and become more important at higher wind and wave conditions. Wind-wave and ocean-swell characteristics are among those parameters which must be monitored for the analytical computation of continental-shelf circulation.

INTRODUCTION

The Federal Ocean Program (ref. 1) has the objective of contributing to the national security, the quality of life, and the general welfare. One major element of the program is concerned with the development of new sources of energy to support the economy. Economic, pollution, and transportation considerations dictate increasing dependence upon "offshore" petroleum. The same considerations lead to the proposed construction of offshore nuclear power plants and port facilities. As a result, increased requirements are imposed on future coastal-zone management activities. The Federal Ocean Program is stimulating increasing emphasis on the studies of marine-related safety and pollution problems associated with the production and transportation of energy supplies. To accomplish these studies, improved experimental, analytical, and monitoring techniques are required because complex physical processes occur over large geographical regions.

Much has been written (ref. 2, for example) concerning the monitoring and prediction of ocean circulation from data measured in space. Generally the philosophy seems to be that the monitoring of sea-surface topography would permit definition of location and magnitude of major geostrophic currents and the monitoring of wind would permit estimation of wind-driven currents. The wind, temperature, and sea-surface topography data would be input to analytical models which would compute subsurface as well as surface-circulation characteristics. Thus, the monitoring of ocean circulation from space would be highly dependent upon analytical modeling as well as upon the measurement of appropriate input parameters.

Reference 3 (p. 258) notes that the winds which cause stress-induced currents (known as wind-driven currents) also cause waves (known as wind-waves). It is well established (refs. 3, p. 256, and 4, p. 588, for example) that currents are induced by ocean-surface waves. Associated with waves is a nonclosed orbital motion in the vertical plane which progresses in the direction of wave advance. The drift associated with forward progression of the orbital motion is known as the wave-induced current (ref. 4, p. 984). Wind-driven surface-current speeds may reach as much as 3 percent of windspeed in deep water, and wind-wave-induced currents may reach 1 percent of windspeed according to reference 3. More recent studies (refs. 5, p. 131, and 6) indicate surface wave-induced currents from wind-waves to be between 1.6 and 3.6 percent of windspeed. In addition to wind-waves, a region may also contain ocean swell, which is wind-waves generated by storms in another location that have propagated into the region. Reference 3 (p. 258) notes that, if ocean swell is running through a region of dead calm, the swell may induce a current. In the deep ocean wave-induced currents have traditionally been considered small, but recent results (refs. 6 and 7) state that they may be significant. Reference 6 further notes that theoretical wave-induced currents are increased in water of finite depth. Thus, it is possible that wave-induced currents are important over those continental-shelf regions in which flow velocities are low in comparison to major ocean currents. One such region is a mid-Atlantic continental shelf between 40° north latitude and Cape Hatteras, North Carolina (34° N). An understanding of the environment of this region is important because construction of offshore nuclear power plants, port facilities, and oil wells have been proposed within this area.

It is the purpose of this report to examine the order of magnitude of the wave-induced currents in a mid-Atlantic continental-shelf region for a variety of weather conditions. The wave-induced currents will be compared with currents caused by other factors to assess relative importance. More specifically, a review of general circulation conditions in the region is first conducted. Next, factors such as Gulf Stream dynamics, tidal currents, wind-driven currents, wind-wave currents, and ocean-swell currents which perturb the general circulation condition are examined for order of magnitude. Actual weather statistics for the region are investigated, and the wind-wave and ocean-swell currents are compared with other currents based on frequency of occurrence. This study is for the purpose of helping define what must be remotely monitored and analytically modeled to assess the circulation environment of the region.

SYMBOLS

A	eddy viscosity coefficient, kilograms/meter-second
a	factor defined by $\left(\frac{2\Omega\rho_w \sin\phi}{A}\right)^{1/2}$, meter^{-1}
C_{15}	wind-stress resistance coefficient at 15 meters above surface of water
D	depth of frictional influence defined by $\pi\left(\frac{A}{\rho_w \Omega \sin\phi}\right)^{1/2}$, meters
d	water-column depth, meters
$F(k)$	two-dimensional wave spectrum, newtons
g	gravitational acceleration, meters/second^2
H	wave height, trough to crest, meters
$\bar{H}$	average wave height, meters
$H_{1/3}$	significant wave height, average of highest one-third of waves, meters
k	wave number, $2\pi/L$, meter^{-1}
L	wave length between successive waves, meters
$\bar{L}$	average wave length, meters
T	wave period between successive waves, seconds
$\bar{T}$	average wave period, seconds
$\bar{U}$	Stokes' wave-induced current, meters/second
u	Ekman wind-drift velocity component perpendicular to wind direction, meters/second
v	Ekman wind-drift velocity component along wind direction, meters/second

V_o — total Ekman wind-drift speed, meters/second

w — windspeed, meters/second

z — coordinate distance perpendicular to water surface measured positive downwards from water surface, meters

α, β — constants defined by equations (2), meters/second

ζ — variable defined by $d - z$, meters

ρ_a — density of air, kilograms/meter^3

ρ_w — density of water, kilograms/meter^3

τ — wind stress on water surface, newtons/meter^2

ϕ — latitude of position, degrees

Ω — angular velocity of Earth, radians/second

ω — wave frequency, $2\pi/T$, radians/second

GENERAL CIRCULATION CONDITIONS

Using the terminology of reference 8 (p. v), static conditions are those circulation properties which are obtained by averaging large amounts of measured data over a long time period (monthly, seasonally, or yearly) so that the effects of higher frequency meteorological and tidal perturbations are eliminated. In most cases, ocean-circulation data are summarized on a seasonally averaged basis. Such data are available (refs. 9 and 10) for the continental-shelf region under study in this investigation. The static circulation magnitudes and patterns are modified by the action of local winds, waves, tides, and the Gulf Stream. These dynamic effects will be considered in a subsequent section.

There are few accurate current measurements in the mid-Atlantic continental-shelf region, the subject of this study (ref. 11, p. 45). The majority of the circulation data has been from inferred trajectories calculated by statistical regression analysis of the beginning and end points of several thousand surface drift bottles and seabed bottom drifters (refs. 9 and 10). Additional data have been collected from random ship drift reports which often suffer from inaccurate navigation fixes (ref. 11, p. 45). The majority of the data collected refers to surface currents. Only a limited amount of bottom-current information is available. Mid-depth current data are almost nonexistent.

Figure 1 illustrates the generally accepted surface-current patterns and velocities in the mid-Atlantic continental-shelf area. Figure 2 shows more detailed surface-circulation patterns on a seasonal basis. The solid arrows represent those patterns inferred by statistical analysis of the end points of large amounts of drift-bottle data. The dashed arrows represent interpolations or extrapolations from the solid arrows or results from a small amount of drift data. Currents toward the southwest predominate except in summer when southerly winds subsequent to periods of low rainfall may cause temporary northerly flowing currents (refs. 10 and 12). Little or no surface shelf water is transported south of Cape Hatteras except during periods of sustained winter winds from the northeast (ref. 11, p. 45).

Figure 3 illustrates the generally accepted bottom-current patterns and velocities in the area (ref. 10, p. 41). Seabed drifter data suggest that the average bottom flow is independent of the surface conditions in the late spring and summer but is more coupled to them in the late fall and winter when the water column is near neutral stability. In spring the temperature of the surface water increases more rapidly than that at the bottom, causing a lower density at the surface and stratification of the water column. The vertical density gradient is further enhanced by the increase in fresh-water discharge from the continent which adds less dense water to the surface layer. Maximum stability, with denser water on the bottom and lighter water on the surface, is reached in the summer when fresh-water discharge is maximum (ref. 10, p. 39). In the autumn fresh-water discharge slackens and seasonal colder temperatures cause thermal stratification to disappear, and the water column becomes neutrally stable, nearly isothermal and isohaline, through the winter (ref. 10, p. 40). Figure 4 shows average bottom-circulation patterns both with and without thermal stratification.

DYNAMIC CIRCULATION CONDITIONS

Dynamic circulation conditions are those perturbations on static conditions which are caused by the effects of Gulf Stream dynamics, tides, waves, and winds. Both local winds and storms in the deep ocean affect continental-shelf circulation. Local winds cause wind-driven currents (due to shear stress) as well as wave-induced currents from the local wind-waves. Deep-ocean storms generate wind-waves offshore which disperse and propagate onto the continental-shelf area as long-period ocean swell. The ocean swell, which is usually independent of local wind conditions, also produces wave-induced currents. Gulf Stream dynamics, tidal currents, wind-driven currents, wind-wave currents, and ocean-swell currents will be considered in the following sections.

Gulf Stream Dynamics

Gulf Stream dynamics may have a significant impact on continental-shelf circulation. The north wall of the Gulf Stream is believed to influence the slope front which is the outer boundary of continental-shelf waters (see fig. 1). The mean position of maximum currents of the Gulf Stream shows little change from season to season (see fig. 5), but the variation of the mean position can be rapid and intense in monthly synopses (ref. 8, p. 692). Figure 5 shows the slope-front positions over a 5-year period on a monthly basis (numbered 1 to 12). Because the positions represent an average for the indicated month, the fluctuations shown may have been quite rapid and only a few days in duration. The slope front appears sometimes to move very close to the New Jersey and New England coasts during the summer and early fall.

Continental-shelf waters originate in the areas above 40° North latitude and flow past Nantucket shoals on their way south along the coast to Cape Hatteras (fig. 1). Close inshore Gulf Stream meanders may temporarily inhibit the supply of shelf waters and perhaps cause a major fluctuation in circulation conditions in the mid-Atlantic regions. The effects of Gulf Stream meanders on shelf circulation are not well understood because synoptic circulation data coinciding with these meanders are not generally available. A better understanding of Gulf Stream dynamics is a prerequisite to the accurate prediction of continental-shelf circulation. Although these meanders are known to be important, the remainder of this study will neglect the effects of Gulf Stream dynamics on shelf circulation since the order of magnitude of these fluctuations is not known.

Tidal Currents

The gravitational forces of the Moon and Sun cause tides in the oceans which in turn create currents. Tidal changes in water level combine with topographical features to give rise to three types of tidal currents: (a) the reversing type, illustrated by currents in most inland bays and rivers, (b) the hydraulic type, illustrated by currents in straits connecting two independent bodies of water, and (c) the rotary type, illustrated by currents in the open ocean and along the sea coast. Offshore, the tidal current changes its direction continually and never comes to a slack because it is not confined to a definite channel. Over a tidal cycle of about 12.5 hours, the current will have set in all directions of the compass; hence it has become known as the tide-induced rotary current.

The displacement caused by the rotary current takes the form of an ellipse on a horizontal plane parallel to the water surface. The direction of rotation is clockwise in the Northern hemisphere. The current is variable with topography and geographical location. The following list shows averaged maximum rotary current speeds for several mid-Atlantic shelf locations (see fig. 1) as taken from reference 13 (pp. 179 and 181):

Location	Depth, m	Speed, cm/sec
① 70 miles east of Cape Charles, Virginia	183.0	10
② 72 miles east of Cape May, New Jersey	54.8	5
③ Five-Fathom Bank Lightship, Delaware	18.3	10
④ Winter Quarter Shoal Lighted Whistle Buoy, Virginia	18.3	5
⑤ Fenwick Shoal Whistle Buoy, Delaware	18.3	15
⑥ Chesapeake Light, Virginia	14.6	Weak

When perigee occurs at or near the time of full Moon, the speeds will be 30 to 40 percent above these averages giving rotary currents up to 21 cm/sec. Apogee occurring at quadrature will cause maximum speeds 30 to 40 percent below average. The magnitude of the currents is comparable to the values of the static surface currents (fig. 1) and is several times larger than static bottom currents (fig. 3). Because of the large values of the tidal current, experimental circulation data are often difficult to interpret when measurements are for less than one tidal cycle. The currents actually observed consist of tidal currents masked by nontidal currents. Considering sequential tidal cycles, there are small variations in the elliptical orbits related to slow changes in phase, parallax, and declination of the Moon. These variations result in the end point of the rotary orbit not precisely matching its beginning point (even when nontidal effects are zero) causing a net tidal drift current over a sequence of tidal cycles. There is little information available on the tidal drift current; however, it is generally considered to be quite small, possibly much less than 1 cm/sec. It is not clear whether tidal drift is an important parameter in the analysis of long-term circulation characteristics of the shelf; however, tidal rotary currents are clearly important for short-duration activities.

Wind-Driven Currents

Wind-driven currents are the result of shear stress applied to the surface of the water by local winds. Pure wind-driven currents are seldom observed in nature since the same local winds that produce them also cause wind-waves. An exception is in Arctic ice packs where the ice sometimes does not allow a sufficient fetch for significant wave generation. For these cases a predominantly pure wind-driven current may exist. Fridtjof Nansen, during the "Fram" Polar Sea expedition (1893-1896), observed that the ice drift deviated 20° to 40° to the right of the wind. At the suggestion of Nansen, V. W. Ekman performed a mathematical analysis of these observations by assuming a simple balance between the Coriolis forces and the frictional forces in the water (ref. 14, p. 492). Best known is his solution for an infinitely deep ocean (also called the Ekman spiral), but Ekman also examined the case of a finite-depth ocean. Reference 15 (p. 191 and following pages) discusses both solutions. The finite-depth solution, used in this analysis, has been applied by Ekman and others to waters of depths comparable to continental-shelf depths.

The major assumptions of the Ekman theory include a homogeneous, horizontally unbounded ocean with a uniform wind field. The current components are unaccelerated, and no vertical current component exists. Also, the current velocity components are zero at the bottom and horizontal pressure gradients do not exist. Under these assumptions, vertical profiles for the pure wind-driven currents are calculated from the following finite-depth Ekman-solution equations (ref. 15, p. 194):

$$\left.\begin{aligned} u &= \alpha \sinh \frac{a}{\sqrt{2}} \zeta \cos \frac{a}{\sqrt{2}} \zeta - \beta \cosh \frac{a}{\sqrt{2}} \zeta \sin \frac{a}{\sqrt{2}} \zeta \\ v &= \alpha \cosh \frac{a}{\sqrt{2}} \zeta \sin \frac{a}{\sqrt{2}} \zeta + \beta \sinh \frac{a}{\sqrt{2}} \zeta \cos \frac{a}{\sqrt{2}} \zeta \end{aligned}\right\} \tag{1}$$

where

$$\zeta = d - z$$

The constants α and β are

$$\left.\begin{aligned} \alpha &= \frac{\tau D}{A\pi} \frac{\cosh \frac{a}{\sqrt{2}} d \cos \frac{a}{\sqrt{2}} d + \sinh \frac{a}{\sqrt{2}} d \sin \frac{a}{\sqrt{2}} d}{\cosh 2 \frac{a}{\sqrt{2}} d + \cos 2 \frac{a}{\sqrt{2}} d} \\ \beta &= \frac{\tau D}{A\pi} \frac{\cosh \frac{a}{\sqrt{2}} d \cos \frac{a}{\sqrt{2}} d - \sinh \frac{a}{\sqrt{2}} d \sin \frac{a}{\sqrt{2}} d}{\cosh 2 \frac{a}{\sqrt{2}} d + \cos 2 \frac{a}{\sqrt{2}} d} \end{aligned}\right\} \tag{2}$$

and

$$a = \sqrt{\frac{2\Omega \sin \phi \rho_w}{A}} \tag{3}$$

and

$$D = \pi \sqrt{\frac{A}{\rho_w \Omega \sin \phi}} \tag{4}$$

The total Ekman wind-driven current may be obtained from

$$V_o = \sqrt{u^2 + v^2} \tag{5}$$

The adequacy of the results, granted the original assumptions, depends also on the values used for the effective eddy viscosity coefficient, A, and the effective wind stress, τ.

The concept of eddy viscosity was first adopted for use in ocean-current studies by Ekman in 1902 (ref. 15, p. 185) as a measure of the degree of oceanic turbulence present. The assumption of a constant eddy viscosity coefficient is inadequate since the coefficient is known to vary as a function of both wind speed and depth. Unfortunately, a precise relationship has not been determined for all conditions. Compounding the problem is the usual presence of other currents that make empirical determination of the eddy viscosity coefficients for pure drift currents seemingly impossible. However, Ekman did derive an empirical relationship between the eddy viscosity coefficient and windspeed based on Nansen's ice-drift observations discussed earlier. In these cases a predominantly pure wind-driven current existed. Thorade in 1914 (ref. 15, p. 210) revised the relationship for windspeeds less than 6 m/sec as follows:

$$\left.\begin{aligned} A &= 1.02\, w^3 \quad \text{for} \quad w < 6 \text{ m/sec} \\ A &= 4.3\, w^2 \quad \text{for} \quad w \geqq 6 \text{ m/sec} \end{aligned}\right\} \tag{6}$$

The relationships obtained are for near-surface waters but, for purposes of this investigation, are applied to the entire water column. No attempt is made to vary the eddy-viscosity coefficients with depth as no definitive information exists on how the coefficients would vary. These assumptions are expected to allow reasonable estimates of the pure Ekman drift surface speed. While not a subject of this study, the directional characteristics with depth of the Ekman current relative to the wind are also subject to differences due to neglecting the depth variation of the eddy-viscosity coefficient (ref. 14, p. 496).

The wind stress is usually expressed in terms of a resistance coefficient, the windspeed at some distance above the sea surface, and the density of air

$$\tau = C_{15}\rho_a w^2 \quad , \tag{7}$$

In this case the resistance coefficient C_{15}, empirically obtained, is applicable to a wind measurement 15 meters above the sea surface. Recent compilation of observed data (ref. 16) has shown the resistance coefficient to be a function of windspeed up to 15 m/sec and a nondimensional constant, 0.0026, thereafter. For this analysis, however, the resistance coefficient has been assumed to have the constant value as quoted in reference 14 (p. 490),

$$C_{15} = 0.0026 \tag{8}$$

This value may cause an overprediction of the pure Ekman currents for windspeeds less than 15 m/sec.

Two continental-shelf depths have been used in the calculations: 18.3 meters (10 fathoms) and 36.6 meters (20 fathoms). These are typical depths for proposed construction of offshore facilities. The wind-driven current-profile calculations were made for a range of wind conditions consisting of Beaufort scale numbers from 2 to 11, the corresponding speeds for which are given in table I as taken from reference 17 (p. D40).

TABLE I.- WINDSPEEDS FOR BEAUFORT SCALE

Beaufort scale	Condition	Windspeed, knots	Windspeed, m/sec
2	Light breeze	5.0	2.6
3	Gentle breeze	10.0	5.1
4	Moderate breeze	14.0	7.2
5	Fresh breeze	19.0	9.8
6	Strong breeze	26.0	13.4
8	Fresh gale	37.0	19.0
10	Whole gale	52.0	26.8
11	Storm	59.5	30.6

Results of the calculation for Ekman wind-driven current-speed profiles are shown in figure 6. The significance of the dashed curve in figure 6(b) will be discussed later. In a comparison of figures 6(a) and 6(b), the magnitude of the calculated wind-driven surface current is a strong function of the water-column depth for the higher windspeeds and values of A and τ used. For the shallower column depth of 18.3 meters, increases in windspeed above 9.8 m/sec cause only a small increase in the wind-driven current speed. For the deeper water-column depth of 36.6 meters, however, the magnitude of the calculated wind-driven current is much higher for winds in the 10 to 20 m/sec range, and the current speed for the maximum wind case of 30.6 m/sec is almost twice as large as for the shallow water depth. Ekman theory, by its original assumptions, will always predict zero current speed at the bottom, but use of alternative laws for the eddy-viscosity coefficient will cause the current magnitude to vary with depth (ref. 14, p. 496). For both of the water depths considered, the results indicate that wind-driven currents are an important factor influencing shelf-circulation dynamics.

Wind-Wave Currents

Waves, whether wind-waves (sea) or ocean swell, cause a near-elliptical orbital motion of the water particles in the vertical plane beneath the wave profile. As noted earlier, the beginning and end points of each orbit do not coincide; hence, there is a slow, progressive advance of the particle orbits as the wave trains pass overhead. The rate at which the orbits advance is known as the wave-induced current (also sometimes called "wave drift" or "Stokes' drift," ref. 4). The current direction is in the same direction as advancement of the surface-wave front. The velocity of the water particles around the orbit (known as the wave-induced orbital velocity) is large in comparison to the drift rate of the orbit (wave-induced current). The wave-induced orbital velocity causes the high-velocity water particles to "scrub" the bottom, throwing sediment particles into suspension which may be transported by wave-induced or other currents.

As has been noted, the same local winds that cause wind-driven currents also produce wind-waves. The wind-waves cause wind-wave induced currents; hence, wind-driven and wind-wave induced currents coexist (along with other types of currents) over the continental-shelf regions. In this analysis the wind-driven and wind-wave-induced currents are considered separately so that some idea of their relative magnitudes is obtainable. The problem of how, in the end, separate current components are combined into a total current is not addressed here.

For purposes of this analysis of wind-wave-induced currents, wind duration and fetch are considered sufficient for a fully aroused sea. While these conditions occur rather infrequently for the high waves (to be discussed later), together they represent a limiting case which is important in the instance of a large storm where the potential for serious damaging effects exists. Under these assumptions, the characteristics for wind-waves are empirically related to the windspeed. Shown in table II is the traditional relation of average wind-wave height and period characteristics (ref. 17, p. D40) for the windspeeds of the Beaufort scale presented earlier.

TABLE II.- WAVE HEIGHTS AND PERIODS FOR BEAUFORT SCALE

Beaufort scale	Windspeed, m/sec	Significant wave height, m	Average wave height, m	Average wave period, sec	Average* wave length, m	Average† wave length, m
2	2.6	0.09	0.05	1.4	3	3
3	5.1	.43	.27	2.9	13	13
4	7.2	1.01	.61	4.0	25	25
5	9.8	2.10	1.31	5.4	45	46
6	13.4	4.58	2.93	7.4	77	85
8	19.0	11.30	7.03	10.5	125	155
10	26.8	26.50	16.50	14.8	187	249
11	30.6	35.40	22.30	17.0	218	295

*Based on average period and 18.3-meter depth.

†Based on average period and 36.6-meter depth.

The average wave lengths for the depths considered are determined iteratively from

$$\bar{L} = \frac{g\bar{T}^2}{2\pi} \tanh\left(\frac{2\pi d}{\bar{L}}\right) \tag{9}$$

where the initial approximation for the average period and wave length are the deep-water conditions.

For a fixed weather condition, wind-wave height characteristics vary in a stochastic manner as a function of wave frequency (or period). A fixed wind will result in a frequency spectrum of wind-wave heights. Marine forecasts and observations usually report the significant wave height, which is the average of the highest one-third waves. The average height of the total wave spectrum will be considerably less than the significant wave height. Ideally, wave-induced currents should be obtained considering the total wave-height spectra as suggested in reference 6. An approximate calculation can be made, however, using average values of wave height and period, as obtained from the preceding table, if order-of-magnitude estimates of wind-wave-induced currents are desired.

For the monochromatic wave, wave-induced currents can be established for open bodies of water using second-order Stokes irrotational theory (refs. 4, p. 984, and 18). Reference 19 concluded that, for deep-water waves, the irrotationality assumption of Stokes is valid. Reference 20 added the restriction of null mass transport and consideration of a bottom boundary layer (rotational flow), which is the case of waves moving in a shallow-confined basin (such as a wave tank). Reference 3 (p. 504) notes that in the open ocean, however, the condition of null mass transport is unlikely. This investigation assumes that second-order Stokes theory is valid for estimating the order of magnitude of wave-induced currents and limits itself to the wave conditions for which Stokes' theory is considered valid. The assumption of irrotationality would cause an underprediction of wave-induced currents on the bottom (ref. 3, p. 510). By Stokes' theory the wave-induced currents are given by (ref. 4, p. 984)

$$\bar{U} = \frac{\pi^2}{2} \frac{\bar{H}^2}{\bar{T}\bar{L}} \frac{\cosh\left(\frac{4\pi(d - z)}{\bar{L}}\right)}{\sinh^2\left(\frac{2\pi d}{\bar{L}}\right)} \tag{10}$$

Stokes' theory is considered valid for waves that fulfill the conditions (ref. 21)

$$\left.\begin{aligned} &\frac{L}{d} \leqq 7.13 \quad \text{for any} \quad \frac{H}{2d} \\ &\frac{L}{d} < 2\pi\sqrt{\frac{8}{3}\frac{d}{H}} \quad \text{for smaller amplitude waves} \quad \frac{H}{2d} < 1.0 \end{aligned}\right\} \tag{11}$$

These criteria insure convergence of the mathematical-series approximations in the theory. Physically, waves will break if the ratio $\frac{H}{2d}$ exceeds about 0.14. This boundary condition is the same as saying that

$$\frac{L}{d} \geqq 7.13\left(\frac{H}{2d}\right) \tag{12}$$

for waves not to break.

These criteria are shown in figure 7, from which it is seen that there exists a roughly triangular area for which Stokes' theory is mathematically convergent and the waves are nonbreaking. Shown in the same figure are the wind-wave conditions of the Beaufort scale. The figure indicates that Stokes' theory should be applicable for average wave values for all Beaufort conditions considered except for Beaufort scale 11 at the 18.3-meter depth. Wind-wave-induced currents produced by average wind-waves are presented in figure 8. In each case, the curves are identified by the average wave height. The significance of the dashed curves will be discussed later. Considering the values for the 18.3-meter depth (fig. 8(a)), it is apparent that wind-wave-induced currents are quite large for wave heights of 2.9 meters or more. Stokes-theory calculations for whole gale conditions (average wave height of 16.5 m) for the 36.6-meter depth (fig. 8(b)) suggest wind-wave-induced surface speeds that are of the same order of magnitude as Gulf Stream surface speeds.

An item of concern, as noted earlier, is the accuracy of results obtained from calculations which use average wave height and length instead of values over the total spectrum. As reference 6 notes, the Stokes wave-induced current for a two-dimensional spectrum and an arbitrary depth is given by

$$\overline{U}(z) = \frac{1}{\rho_W}\iint_{-\infty}^{\infty} F(k)\frac{k}{\omega(k)}\left[\frac{2k \cosh 2k(d - z)}{\sinh 2kd}\right]dk \tag{13}$$

where $F(k)$ is an assumed two-dimensional wave spectrum and the wave frequency ω is related to the wave number by

$$\omega^2 = gk \tanh kd \tag{14}$$

Unfortunately, weather statistics are not compiled on a wave-spectrum basis nor is there sufficient information available for their exact computation. Thus, studies of wave-induced currents using equation (13) are made on the basis of assumed semiempirical wave spectra. Detailed study of figure 9 offers some insight into the spectrum versus average wave-height approaches. The solid curves represent Stokes' surface wind-wave-induced currents for the 18.3-meter, 36.6-meter, and 5500-meter depths computed using average values. Wind-speed values were obtained by correlation of $\bar{\bar{H}}$ with windspeed for the previous table which assumes fully aroused seas. Current values for the 18.3-meter and 36.6-meter depths were taken directly from figure 8. As suggested in reference 6, it is seen that the shallow continental-shelf depths cause increased wind-wave-induced currents. The dotted line represents the wind-wave-induced current magnitudes estimated for the deep ocean by reference 3 (1.0 percent of windspeed). The wind-wave-induced currents shown by the dashed lines (1.6 to 3.6 percent of windspeed with 1.6 percent preferred) were computed in reference 6 using equation (13) and two semi-empirical spectra using different assumed profiles. Reference 3 does not indicate a windspeed range for its 1.0-percent value, but the analysis in reference 6 was limited to windspeeds between 10 m/sec and 20 m/sec. The average wave height and length approach of this study for the deep ocean, 5500-meter depth, underpredicts the 1.0-percent line for windspeeds less than 14 m/sec and overpredicts it above 14 m/sec. It also underpredicts the preferred 1.6-percent value in the 10-m/sec to 20-m/sec range. Unfortunately, open-ocean wind-wave-induced current data are unavailable, so a direct comparison with the experimental results is not possible for any of the curves. It appears, however, that the method of this study does give reasonable order-of-magnitude estimates in the deep ocean and is appropriate for calculations on the continental shelf. It is indicated from figure 8 that wind-wave-induced currents are a major factor influencing continental-shelf circulation.

Ocean-Swell Currents

Ocean swell represents those waves which were originally generated by a deep-ocean storm rather than by the local wind. Originally these waves were part of a wind-wave spectrum. As the wind-wave spectrum propagated outside the storm region, the spectrum began to separate because longer length waves travel faster than short waves. Lateral dispersion, winds, and viscosity cause the waves to decay as they propagate across the deep ocean. As a result, the ocean swell that reaches the continental shelf is usually long-period and low-to-moderate in height. Because the swell spectrum is dispersed over distance, the swell observed at a particular location and time will have nearly monochromatic characteristics based on physical theory. In reality, the situation is somewhat more complex, but recent photographic observations (ref. 22) tend to confirm the near-monochromatic nature of the ocean swell. Both photographs and coastal-wave records suggest that the continental shelf may simultaneously receive several ocean-swell trains from different directions which originated from separate storms in different parts of the ocean.

Typical statistics for the height of ocean swell in the region of interest may be obtained from reference 8 (p. 199). Little information appears to be published concerning pure swell periods in the region of interest although some data are available concerning combined sea and swell period statistics (ref. 23, p. 012). Swell period is usually larger than that of the local wind-waves. For purposes of this investigation, swell periods of 7, 11, and 17 seconds are assumed over the height range given in reference 8 to approximately bracket possible swell periods from the information given in reference 23 (p. 012). Specific conditions used for calculations are given in table III.

TABLE III.- OCEAN-SWELL CHARACTERISTICS USED FOR CALCULATIONS

Swell height, m	Swell period, sec	Swell length,* m	Swell length,† m
0.16	7, 11, 17	71, 132, 218	76, 166, 295
.88	7, 11, 17	71, 132, 218	76, 166, 295
1.86	7, 11, 17	71, 132, 218	76, 166, 295
2.85	7, 11, 17	71, 132, 218	76, 166, 295
3.66	7, 11, 17	71, 132, 218	76, 166, 295
4.88	7, 11, 17	71, 132, 218	76, 166, 295

*Based on 18.3-meter depth.
†Based on 36.6-meter depth.

The swell lengths were computed using equation (9). Second-order Stokes theory (eq. (10)) is used to compute the swell-induced current speeds. In this case, swell is assumed nearly monochromatic in character, and thus the problem of whether to use the average-wave-height form of analysis (eq. (10)) or the wave-spectrum analysis (eq. (13)) is avoided. Applying equations (11) and (12) to the swell statistics presented in the preceding table indicates that Stokes' theory is applicable in all cases considered and that all computed waves are convergent and nonbreaking. Figure 10 presents the calculated values of the speed profiles for the swell-induced currents. The significance of the dashed curves will be discussed later. Figures 10(a) through 10(c) are for the 18.3-meter water-column depth and show that lengthening of swell period (and wave length) causes increased swell-induced speeds at the bottom and decreased values on the surface. Figures 10(d) through 10(f) indicate that the effect of the deeper water-column depth of 36.6 meters is a large reduction in ocean-swell currents on the bottom but only a relatively small change in surface speeds from the shallow water, 18.3 meters, situation. Theoretically, the wave-induced currents caused by ocean swell propagating into the shelf are of the same order of magnitude as the wind-driven currents and must be considered as an important factor influencing shelf-circulation dynamics.

DISCUSSION

In order to bring the theoretical dynamic-circulation calculations into perspective, it is necessary to examine the weather conditions which occur over the region of this study.

Wind Conditions

Wind data for the region have been compiled statistically and are published in reference 8 (p. 73). The statistics are compiled on an annual frequency-of-occurrence basis and are presented in figure 11. Comparing summer and winter conditions, the windspeeds during the winter are larger due to the more intense atmospheric pressure cells that usually are characteristic of winter months. Considering winter conditions, the wind is below 23.1 m/sec 99 percent of the time. It must be noted that compilation of weather statistics on a percentage-of-time basis usually does not accurately describe severe storm conditions. Severe storms occur infrequently and are of short duration. As a result, severe-storm statistics are usually given in terms of maximum conditions which might be expected to occur over a period of several years. Reference 8 (p. 324) indicates that over a 5-year interval, a maximum wind of 49.0 m/sec may be anticipated. This value is twice the magnitude of the 99-percentile winter-wind statistic.

Directional characteristics of the wind are quite dynamic. As air-mass fronts pass through the area, wind direction often swings through the entire compass over a weekly or biweekly period. The constantly changing direction of the wind is an important factor influencing shelf-circulation dynamics. Averaging the wind data over monthly intervals tends to eliminate the dynamics but shows prevailing characteristics. For all months of the year, reference 8 (p. 168) shows winds from all directions in the region, but prevailing winds are from the northwest in winter and from the southwest in summer.

The wind statistics from figure 11 may be combined with the theoretical calculations shown in figure 6 to estimate the frequency of occurrence of various magnitudes of wind-driven currents at various depths. Considering that the accuracy of this study is limited by the uncertainty in theoretical calculations, it is not feasible to correlate weather conditions with theory in great statistical detail. For purposes of this study, it is assumed sufficient to compare relative magnitudes of various current components at the 66- and 99-percentile frequencies of annual occurrence at each of the depths of this study. Relative magnitudes during severe storms are not estimated.

Wind-Wave Conditions

The wind-waves are generated by the local wind and, therefore, exhibit similar dynamic characteristics. For low windspeeds, the duration and/or fetch-length values needed for fully arisen wind-wave conditions are low enough that the condition may often exist. For example, reference 17 (p. 42) indicates that, for windspeeds less than 9.8 m/sec (the 66-percentile value from fig. 11), a duration of less than 9 hours or a fetch length of less than 65 n. mi. is enough for fully aroused conditions. For the 99-percentile situation (windspeed less than or equal to 23.1 m/sec), a duration of about 55 hours or a fetch length of about 1000 n. mi. is required. From these values, it is concluded that the previous assumption of fully aroused conditions for computation of the wind-waves is reasonably valid at low wind conditions but somewhat more questionable at the higher speeds because of the constantly changing wind direction and magnitudes on the shelf. Actual wind-wave statistics are given in reference 8 (p. 94) and are presented in figure 11. Similar to the wind, worst-case conditions occur in the winter. From these statistics, $H_{1/3}$ is expected to be less than 6.4 meters 99 percent of the time. Values for the severe storm over a 5-year period are not available, but the maximum winter $H_{1/3}$ expected for a 1-year period is 18.3 meters from reference 8. It is not clear why the maximum wave height is three times larger than the 99-percentile value when the difference between the 99-percentile and maximum winds was only a factor of 2. Infrequent conditions near the fully aroused situation or wave refraction with the continental-shelf bottom topography are possible causes for the inconsistent statistics.

To relate $H_{1/3}$ statistics to the average wave calculations of figure 8, the following relation is used (ref. 17, p. 29):

$$\bar{H} = 0.625H_{1/3} \tag{15}$$

Given $\bar{H}$, it is assumed that average wave lengths exist consistent with the assumption of a fully aroused sea. Only those wind-wave conditions consistent with the 66- and 99-percentile frequency of annual occurrence will be used in the comparison of current magnitudes, as discussed previously.

Ocean-Swell Conditions

Ocean swell represents those waves propagated into an area from a distant storm and, hence, can be distinguished from the local wind-waves. As discussed previously, reference 8 (p. 199) gives seasonal swell-height statistics which are presented in figure 11. Reference 8 does not give complete frequency-of-occurrence statistics. For purposes of this study, a smooth curve was fitted through the given data to obtain values over the entire frequency-of-occurrence range. For example, in the winter period, reference 8 gives swell height less than 1.8 meters for 55 percent of the time and below 3.7 meters for 90 percent of the time. A smooth curve was then fitted through the 0-, 55-, and 90-percentile points and extrapolated to the 99-percentile value of swell height less than or equal to 4.88 meters. A similar process was used for the summer statistic based on points at the 0-, 72-, and 96-percent locations. Review of the long-wave-period data in reference 23 (p. 012) suggests that the extrapolation to 99 percent gives realistic values. Reference 23 gives only 5-year statistics; hence, annualized data cannot be extracted. Maximum swell height experienced over the 5-year period between 1963 and 1968 in the Norfolk, Virginia, region was about 9.8 meters (period between 8 and 13 sec). The maximum value will not be used in the comparison of relative magnitudes of currents, as discussed previously.

Relative Magnitude of Currents

The magnitude of the various currents which contribute to continental-shelf circulation may now be collected in a consistent manner. For purposes of this study, only the worst-case winter conditions are analyzed. The magnitude of the wind- and wave-induced currents would be somewhat lower in the summer (except in storms). The 66- and 99-percentile statistics are taken from figure 11 and applied to figures 6, 8, and 10. Where initial calculations did not match weather statistics, additional calculations were made and plotted as dashed curves in figures 6, 8, and 10. The magnitudes of continental-shelf circulation components are summarized in table IV for the 18.3-meter depths. The static circulation values are those values discussed previously, taken from statistical correlation of drifter data. Gulf Stream dynamics and tidal currents have also been

TABLE IV.- RELATIVE CURRENT MAGNITUDES FOR 18.3-METER DEPTH

Location	Static circulation, cm/sec	Dynamic circulation, cm/sec				
		Gulf Stream dynamics	Tidal currents	Wind-driven currents	Wind-wave currents	Ocean-swell currents
	66% frequency of occurrence					
Surface	5 to 20	Unknown	0 to 21 daily, <1 long-term drift	0 to 13	0 to 5	0 to 10
Bottom	0 to 2			0	0	0 to 2
	99% frequency of occurrence					
Surface	5 to 20	Unknown	0 to 21 daily, <1 long-term drift	0 to 14	0 to 24	0 to 51
Bottom	0 to 2			0	0 to 4	0 to 10

discussed previously. Considering the other factors in the 99-percentile situation, wave-induced currents from both the wind-waves and ocean swell may become larger at times than the currents from other factors which influence circulation. For the more frequent 66-percentile case, the wave-induced currents are much reduced; however, ocean-swell currents are still similar in magnitude to wind-driven currents. Comparison of the 66- and 99-percentile values indicates that wave-induced currents become more important at higher wind and wave conditions.

The relative magnitudes among the various currents are altered when the water-column depth is changed. Relative magnitudes for the 36.6-meter depth are summarized in table V. Deeper depth causes wind-driven currents to increase significantly for both

TABLE V.- RELATIVE CURRENT MAGNITUDES FOR 36.6-METER DEPTH

Location	Static circulation, cm/sec	Dynamic circulation, cm/sec				
		Gulf Stream dynamics	Tidal currents	Wind-driven currents	Wind-wave currents	Ocean-swell currents
	66% frequency of occurrence					
Surface	5 to 20	Unknown	0 to 21 daily, <1 long-term drift	0 to 19	0 to 5	0 to 9
Bottom	0 to 2			0	0	0 to 1
	99% frequency of occurrence					
Surface	5 to 20	Unknown	0 to 21 daily, <1 long-term drift	0 to 27	0 to 18	0 to 45
Bottom	0 to 2			0	0 to 1	0 to 3

percentile values. Surface values for wind-wave and ocean-swell currents are reduced by a small amount. Bottom values for the wind-wave currents are significantly reduced, but ocean swell is still important at the 36.6-meter depth. Wave-induced currents become smaller in comparison to wind-driven currents as the water-column depth becomes larger. It must be again noted, however, that severe storms would significantly alter the relationship shown in the foregoing tables.

It is of some interest to examine the bottom values for the wave-induced currents. The calculated values offer one possible explanation for a phenomenon observed in experimental data. Reference 10 (p. 32) states that bottom static-circulation values (fig. 3) were obtained from averages of a large number of seabed drifters; however, there were a low number of seabed-drifter results which were not included in the averaging process because large deviations from the average were observed. In some cases, the data were believed to be accurate because the drifters were picked up in fishing nets only a short time after they were dropped. The interesting fact about these particular results is that the velocities calculated were a factor of 2 or 3 larger than the static averages. It was concluded that there were transient nontidal effects which caused high bottom velocities. The calculated values for wave-induced currents suggest that transient combinations of wind-waves and ocean swell (as well as refraction effects) could cause the high bottom velocities which were observed. Many oceanographers (ref. 24, for example) believe that wave-induced currents are important in the distribution and dispersal of bottom sediment on the continental shelf. The calculated results from this study tend to confirm that belief.

It must be emphasized that the results of this study do not apply to a specific site. At a specific site, refraction effects may radically increase or decrease wave-induced currents (particularly those from ocean swell). Refraction alters the wave height, and wave-induced currents are proportional to the square of height. Thus, a particular site on the continental shelf may experience either greater or lesser magnitudes of wave-induced currents than are indicated in this study.

While the accuracy of this study is limited to the uncertainties of theoretical calculations, the importance of wave-induced currents in different weather conditions and depths has been assessed. Theoretical results indicate that ocean surface-wave characteristics must be monitored during shelf-circulation experiments if an understanding of shelf processes is to be obtained. Detailed open-water shelf experiments which can be used to test the validity of wind-driven and wave-induced current calculations are not yet available. If analytical models are to be developed for computing subsurface circulation from remote sensing measurements, detailed experimental data are a requirement to test modeling assumptions. Considering the longer term, study results indicate that surface wind-wave and swell characteristics are among those parameters which should be monitored if circulation is to be obtained. In the continental-shelf region (perhaps the deep ocean as well), for the models into which remote sensing data are input to calculate circulation, the wave-induced current effects should be included.

CONCLUDING REMARKS

The importance of wave-induced currents in different weather conditions and water depths (18.3 m and 36.6 m) has been assessed in a mid-Atlantic continental-shelf region. First, a review of general circulation conditions has been conducted. Next, factors which perturb the general circulation condition are examined. Effects of Gulf Stream dynamics and tidal currents are reviewed. Wind-driven currents are estimated using finite-depth Ekman theory for a variety of wind conditions. Wind-wave and ocean-swell currents are calculated using second-order Stokes theory for wave-induced currents for a range of conditions. Actual wind and wave statistics for the region are examined and, finally, the relative magnitudes of the various currents are compared on a frequency of annual occurrence basis.

Results indicate that wave-induced currents are often the same order of magnitude as other currents in the region. At both depths studied, wave-induced currents become particularly important at the higher wind and wave conditions. As water depth increases from 18.3 meters to 36.6 meters, wind-driven surface currents increase and wave-induced surface currents decrease slightly. Wave-induced currents on the bottom are significantly reduced by deeper depth, however. The relative magnitudes of the various currents suggest wind-wave and ocean-swell characteristics are among those parameters which must be monitored for the analytical computation of continental-shelf circulation.

Langley Research Center,
National Aeronautics and Space Administration,
Hampton, Va., October 1, 1974.

REFERENCES

1. Anon.: The Federal Ocean Program. U.S. Govt. Printing Office, Apr. 1973.
2. Apel, John R.: A Hard Look at Oceans From Space. AIAA Paper No. 73-11, Jan. 1973.
3. Kinsman, Blair: Wind Waves – Their Generation and Propagation on the Ocean Surface. Prentice-Hall, Inc., c.1965.
4. Fairbridge, Rhodes W., ed.: The Encyclopedia of Oceanography. Encyclopedia of Earth Sciences Series, Volume I. Reinhold Pub. Corp., c.1966.
5. Kraus, E. B.: Atmosphere-Ocean Interaction. Clarendon Press (Oxford), 1972.
6. Kenyon, Kern E.: Stokes Drift for Random Gravity Waves. J. Geophys. Res., vol. 74, no. 28, Dec. 20, 1969, pp. 6991-6994.
7. Bye, John A. T.: The Wave-Drift Current. J. Mar. Res., vol. 25, no. 1, Jan. 15, 1967, pp. 95-102.
8. Interagency AD HOC Task Force: Environmental Conditions Within Specified Geographical Regions – Offshore East and West Coasts of the United States and in the Gulf of Mexico. Nat. Data Buoy Center, U.S. Dep. Com., Apr. 1973.
9. Bumpus, Dean F.; and Lauzier, Louis M.: Surface Circulation on the Continental Shelf Off Eastern North America Between Newfoundland and Florida. Serial Atlas of the Marine Environment, Folio 7, Amer. Geogr. Soc., 1965.
10. Harrison, W.; Norcross, J. J.; Pore, N. A.; and Stanley, E. M.: Circulation of Shelf Waters Off The Chesapeake Bight, Surface and Bottom Drift of Continental Shelf Waters Between Cape Henlopen, Delaware, and Cape Hatteras, North Carolina, June 1963 – December 1964. ESSA Prof. Paper 3, U.S. Dep. Com., July 1967.
11. Anon.: Environmental Guide to the Virginia Capes Operating Area. SP-211, U.S. Naval Oceanogr. Office, Mar. 1973.
12. Bumpus, Dean F.: Reversals in the Surface Drift in the Middle Atlantic Bight Area. Deep-Sea Res. & Oceanog. Abstr., suppl. to vol. 16, Aug. 1, 1969, pp. 17-23.
13. Anon.: Tidal Current Tables, 1973, Atlantic Coast of North America. Nat. Ocean Surv., U.S. Dep. Com., 1972.
14. Sverdrup, H. U.; Johnson, Martin W.; and Fleming, Richard H.: The Oceans – Their Physics, Chemistry, and General Biology. Prentice-Hall, Inc., 1942.
15. Neumann, Gerhard; and Pierson, Willard J., Jr.: Principles of Physical Oceanography. Prentice-Hall, Inc., c.1966.

16. Wu, Jin: Wind Stress and Surface Roughness at Air-Sea Interface. J. Geophys. Res., vol. 74, no. 2, Jan. 15, 1969, pp. 444-455.

17. Anon.: Shore Protection, Planning and Design. Tech. Rep. No. 4, Coastal Eng. Res. Center, U.S. Army Corps Eng., June 1966. (Available from DDC as AD 750 451.)

18. Stokes, George Gabriel: Mathematical and Physical Papers, Vol. 1. Cambridge Univ. Press, 1880.

19. Huang, Norden E.: Mass Transport Induced by Wave Motion. J. Mar. Res., vol. 28, no. 1, Jan. 15, 1970, pp. 35-50.

20. Longuet-Higgins, M. S.: Mass Transport in Water Waves. Phil. Trans. Roy. Soc. London, ser. A, vol. 245, no. 903, Mar. 31, 1953, pp. 535-581.

21. Laitone, E. V.: Limiting Conditions for Cnoidal and Stokes Waves. J. Geophys. Res., vol. 67, no. 4, Apr. 1962, pp. 1555-1564.

22. Harris, D. Lee: Characteristics of Wave Records in the Coastal Zone. Waves on Beaches and Resulting Sediment Transport, R. E. Meyer, ed., Academic Press, 1972, pp. 1-51.

23. Anon.: Summary of Synoptic Meteorological Observations – North American Coastal Marine Areas. Volume 3: Area 8 – Norfolk, Area 9 – Cape Hatteras, Area 10 – Charleston. U.S. Naval Weather Service Command, May 1970. (Available from DDC as AD 707 700.)

24. Swift, Donald J. P.: Implications of Sediment Dispersal From Bottom Current Measurements; Some Specific Problems in Understanding Bottom Sediment Distribution and Dispersal on the Continental Shelf – A Discussion of Two Papers. Shelf Sediment Transport: Process and Pattern, Donald J. P. Swift, David B. Duane, and Orrin H. Pilkey, eds., Dowden, Hutchinson, & Ross, Inc., c.1972. pp. 363-371.

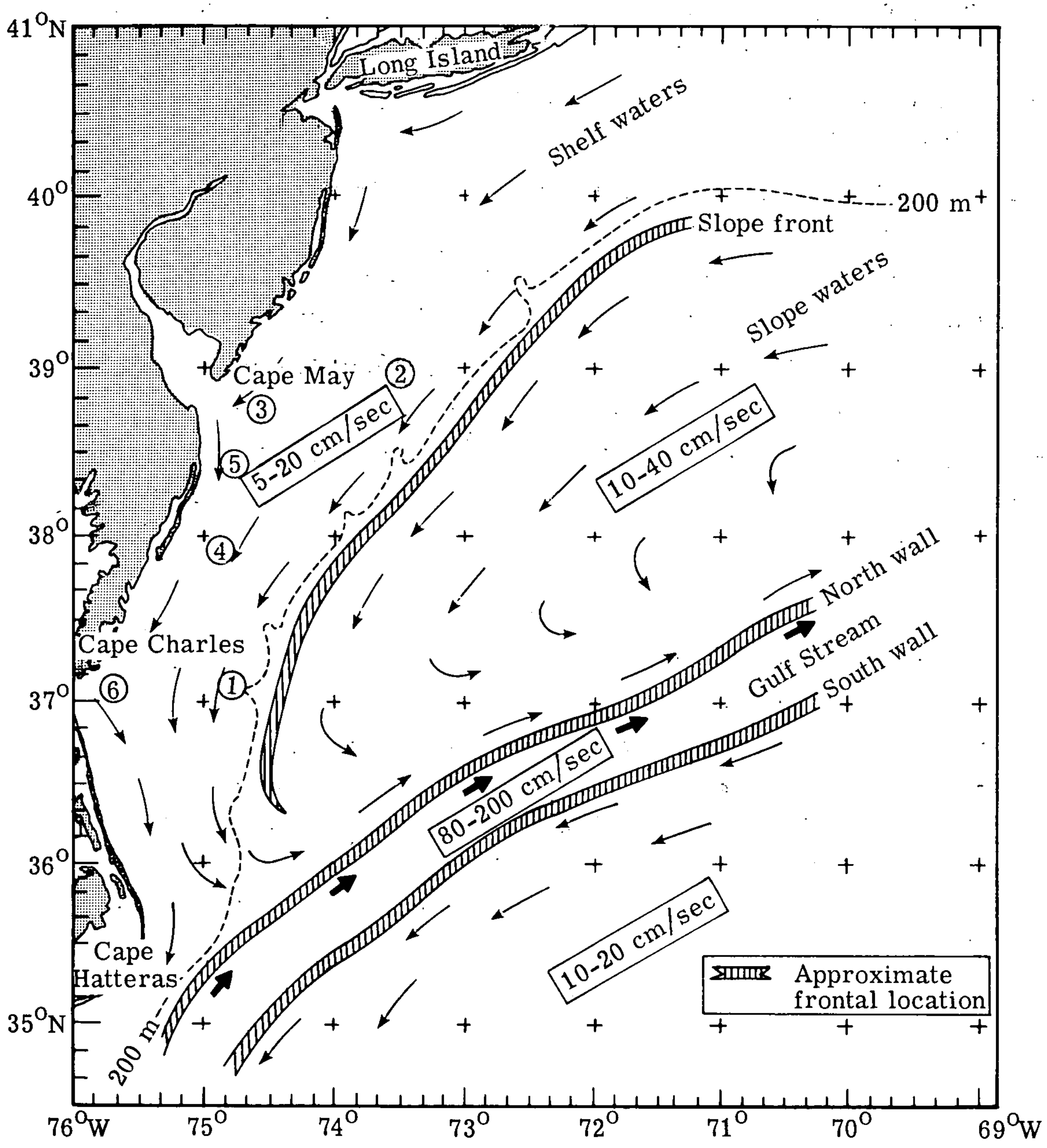

Figure 1.- General surface circulation of the mid-Atlantic continental-shelf region (ref. 11). (Circled numbers are tidal stations referred to in text.)

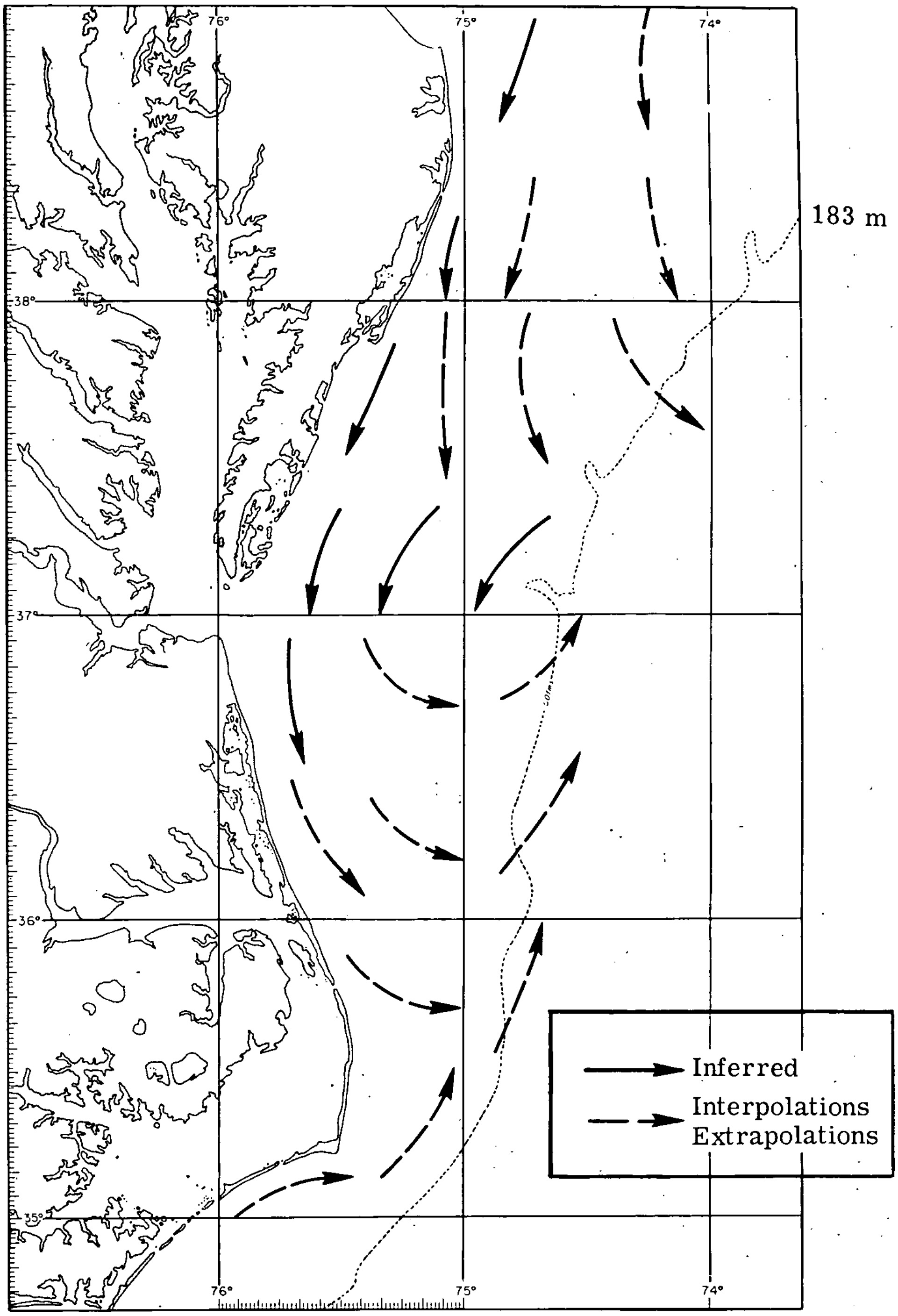

(a) Winter.

Figure 2.- Average surface-circulation patterns (refs. 9 and 10).

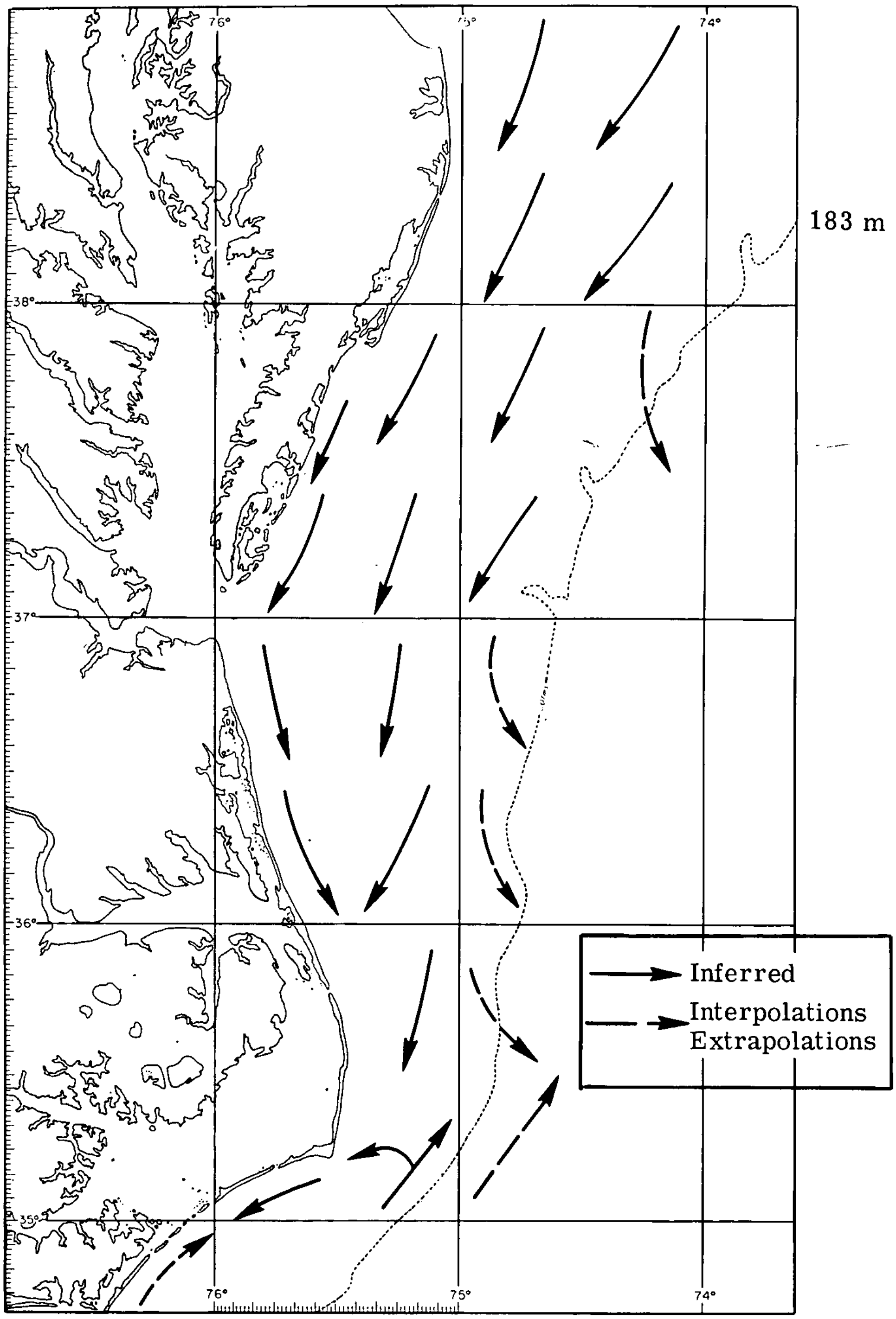

(b) Spring.

Figure 2.- Continued.

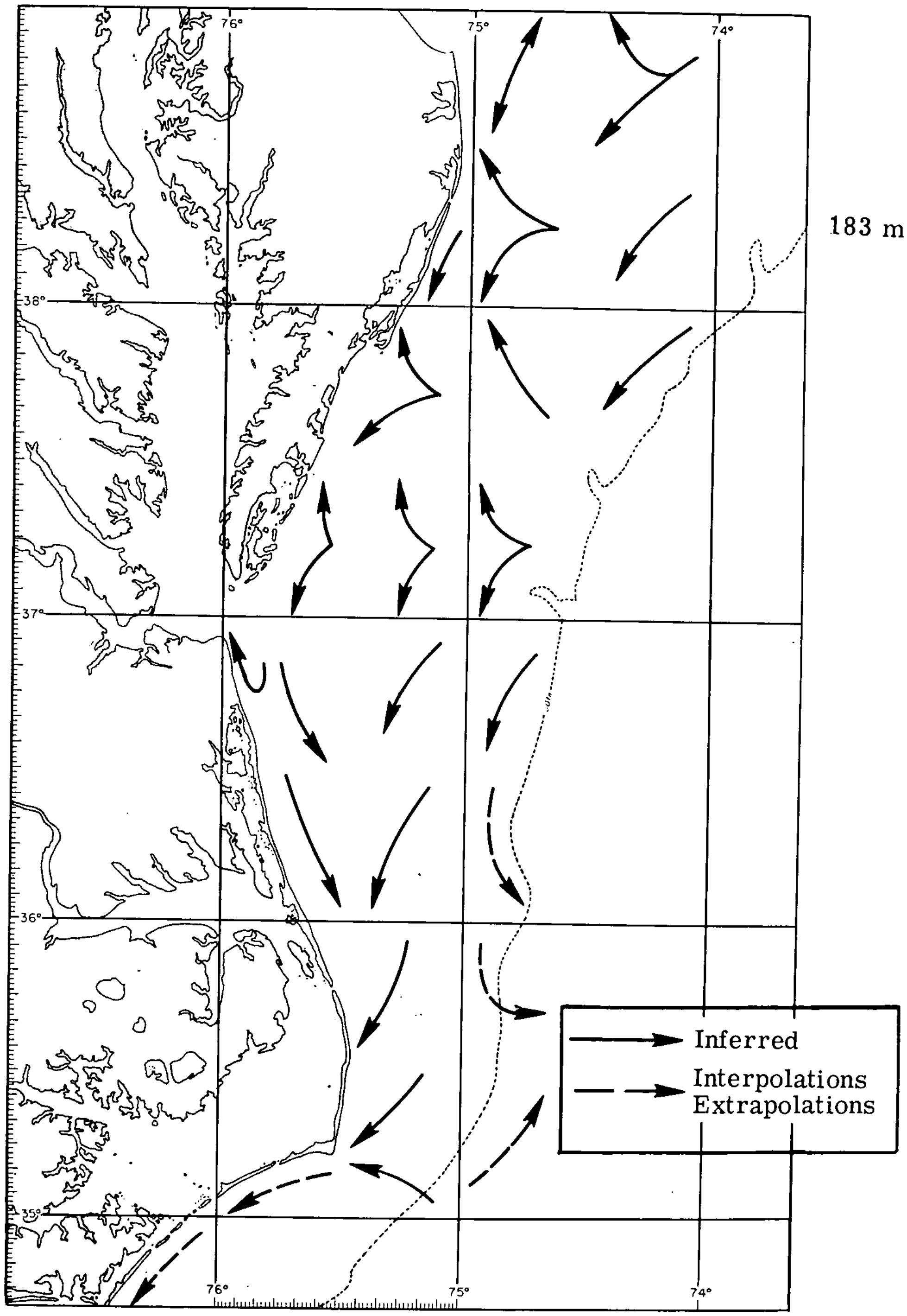

(c) Summer.

Figure 2.- Continued.

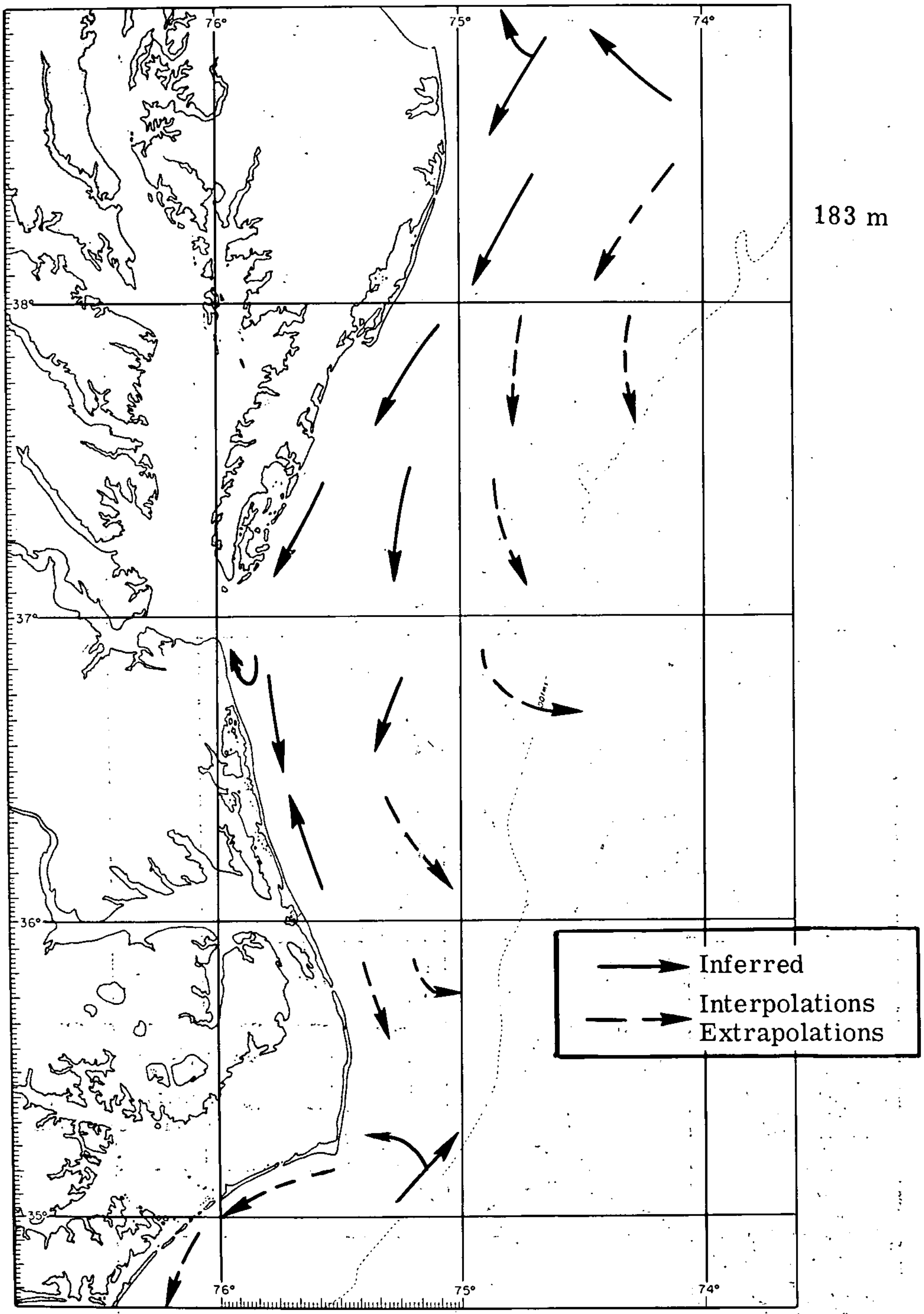

(d) Fall.

Figure 2.- Concluded.

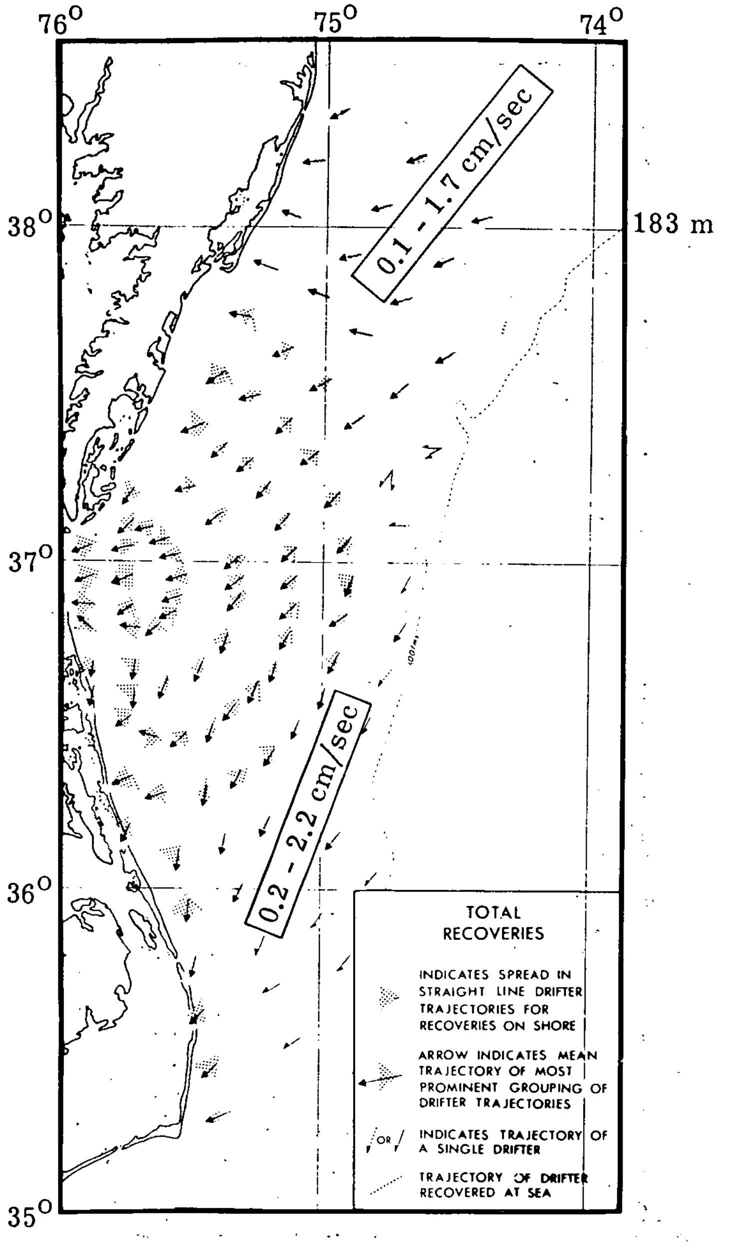

Figure 3.- General bottom circulation of the mid-Atlantic continental-shelf region (ref. 10).

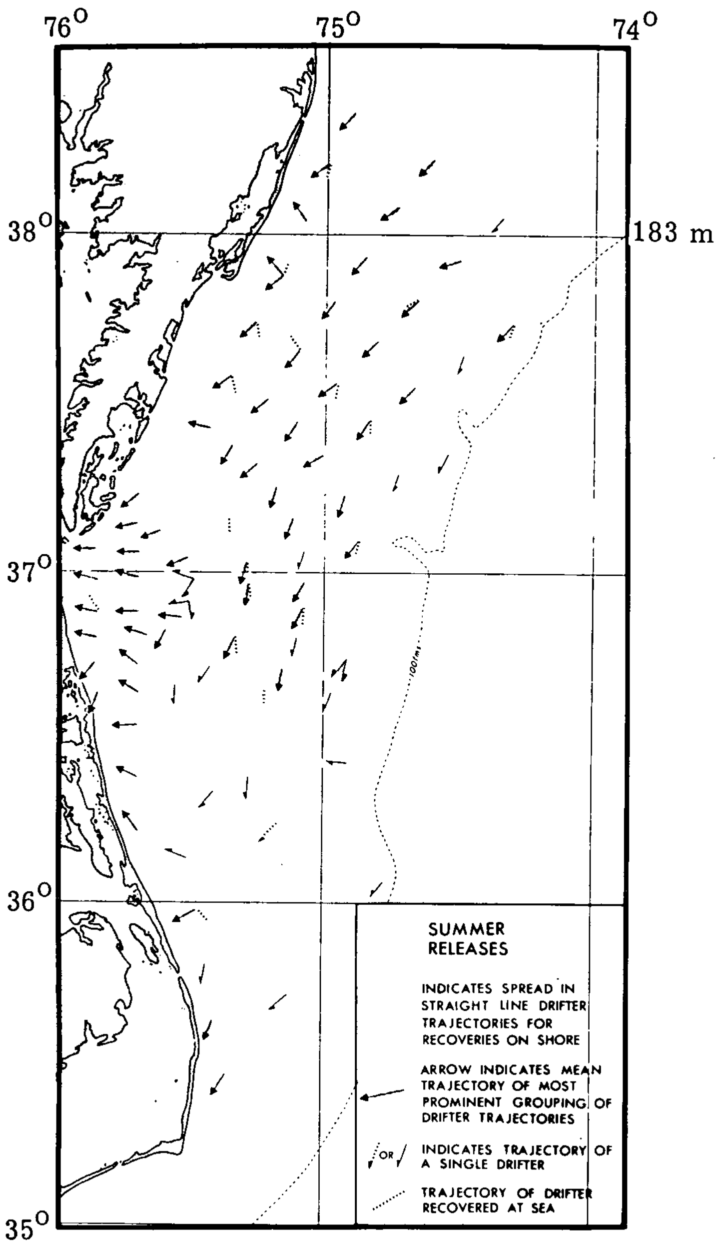

(a) With thermal stratification (summer).

Figure 4.- Average bottom-circulation patterns (ref. 10).

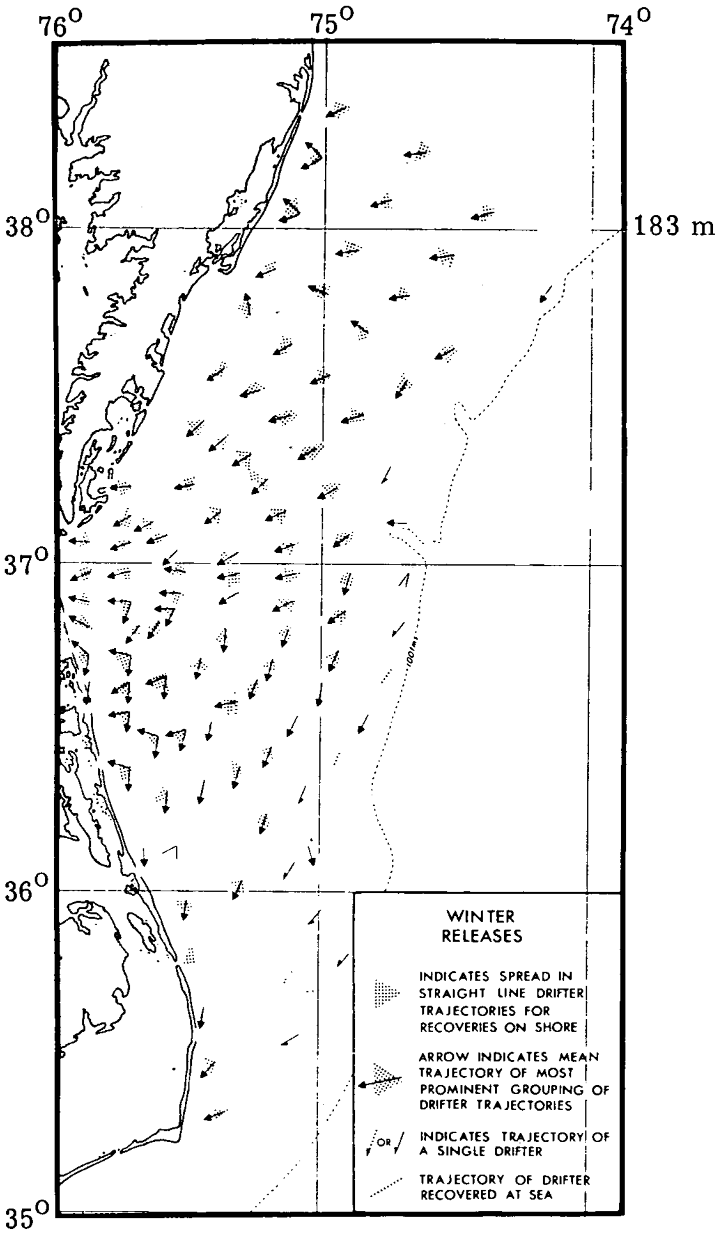

(b) Without thermal stratification (winter).

Figure 4.- Concluded.

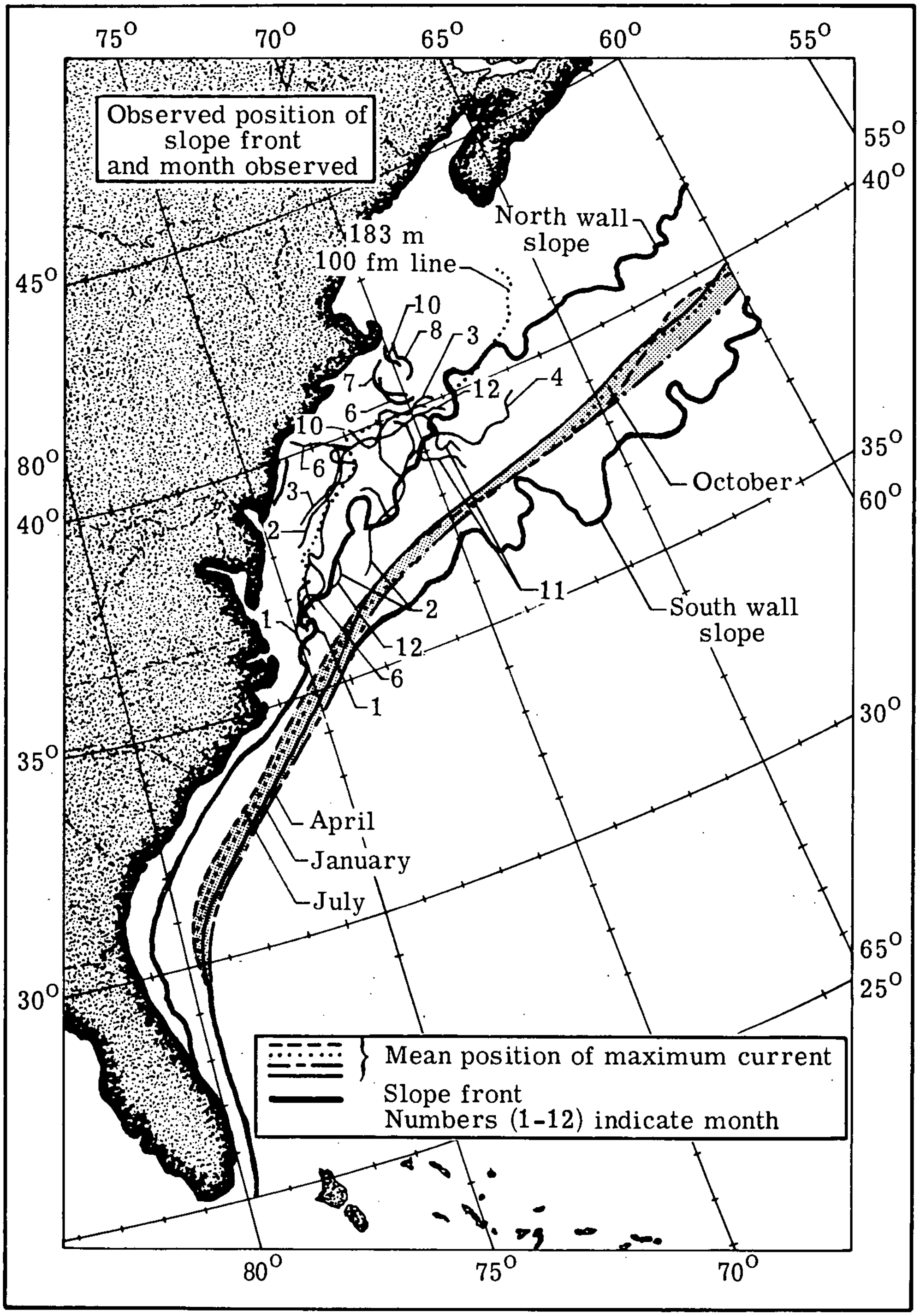

Figure 5.- Gulf Stream meander dynamics (ref. 8).

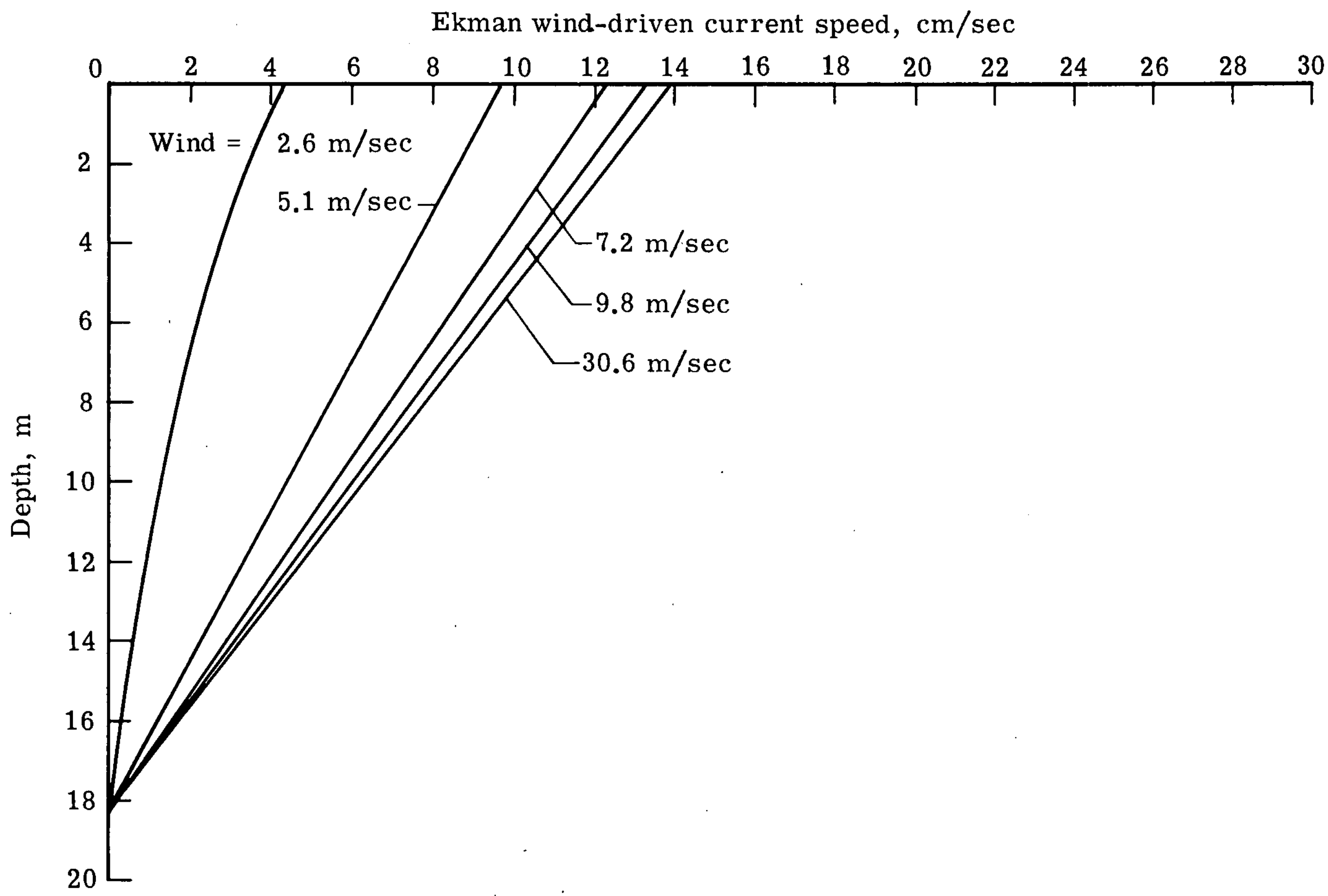

(a) Water depth, 18.3 meters.

Figure 6.- Ekman wind-driven current-speed profiles. (Equations from ref. 15.) (Solid lines represent Beaufort wind conditions, and dashed line represents other conditions.)

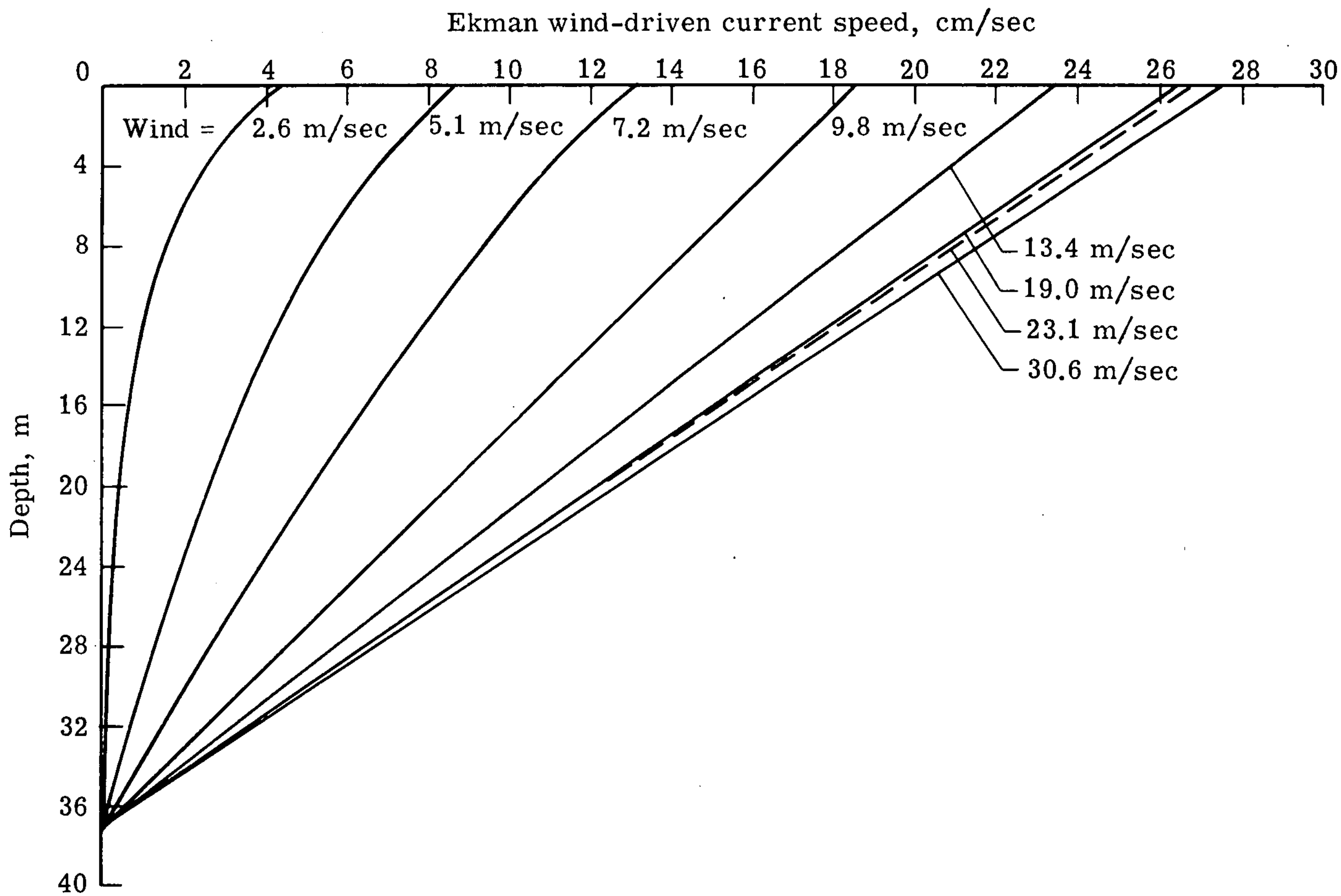

(b) Water depth, 36.6 meters.

Figure 6.- Concluded.

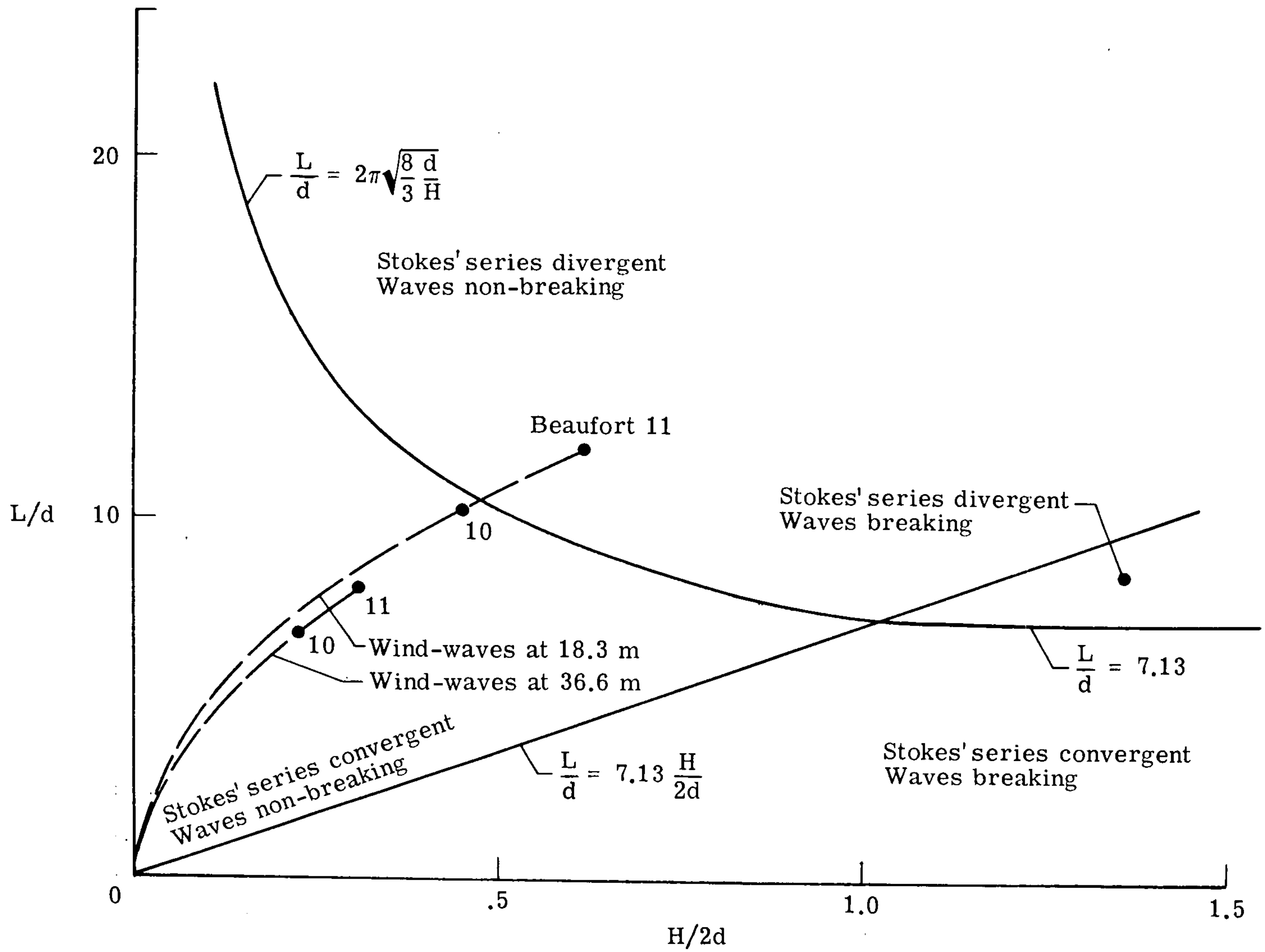

Figure 7.- Limits of applicability of Stokes' theory.

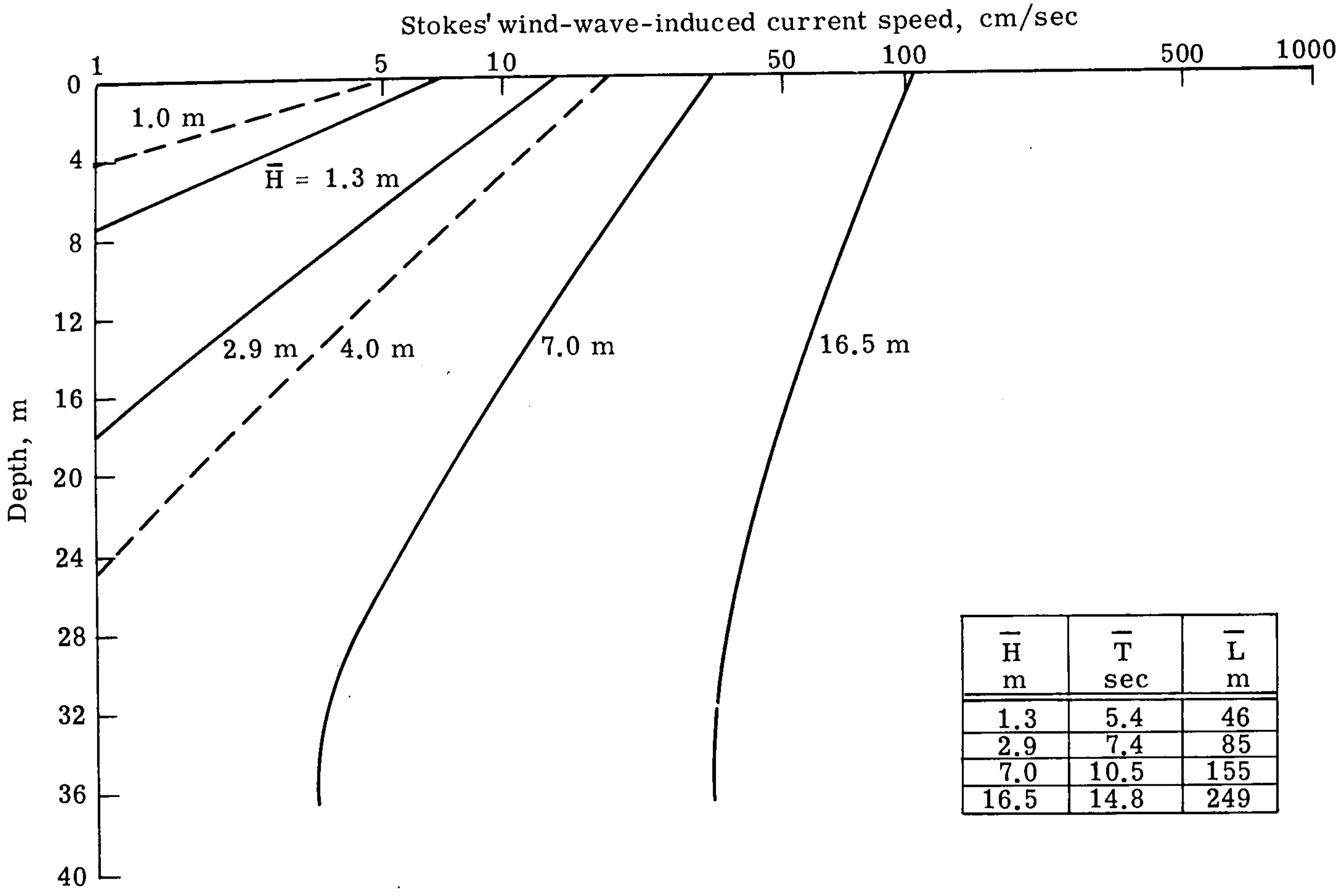

$\bar{H}$ m	$\bar{T}$ sec	$\bar{L}$ m
1.3	5.4	46
2.9	7.4	85
7.0	10.5	155
16.5	14.8	249

(a) Water depth, 18.3 meters.

Figure 8.- Stokes' wind-wave current velocity profiles. (Solid lines represent Beaufort wind conditions, and dashed lines represent other conditions.)

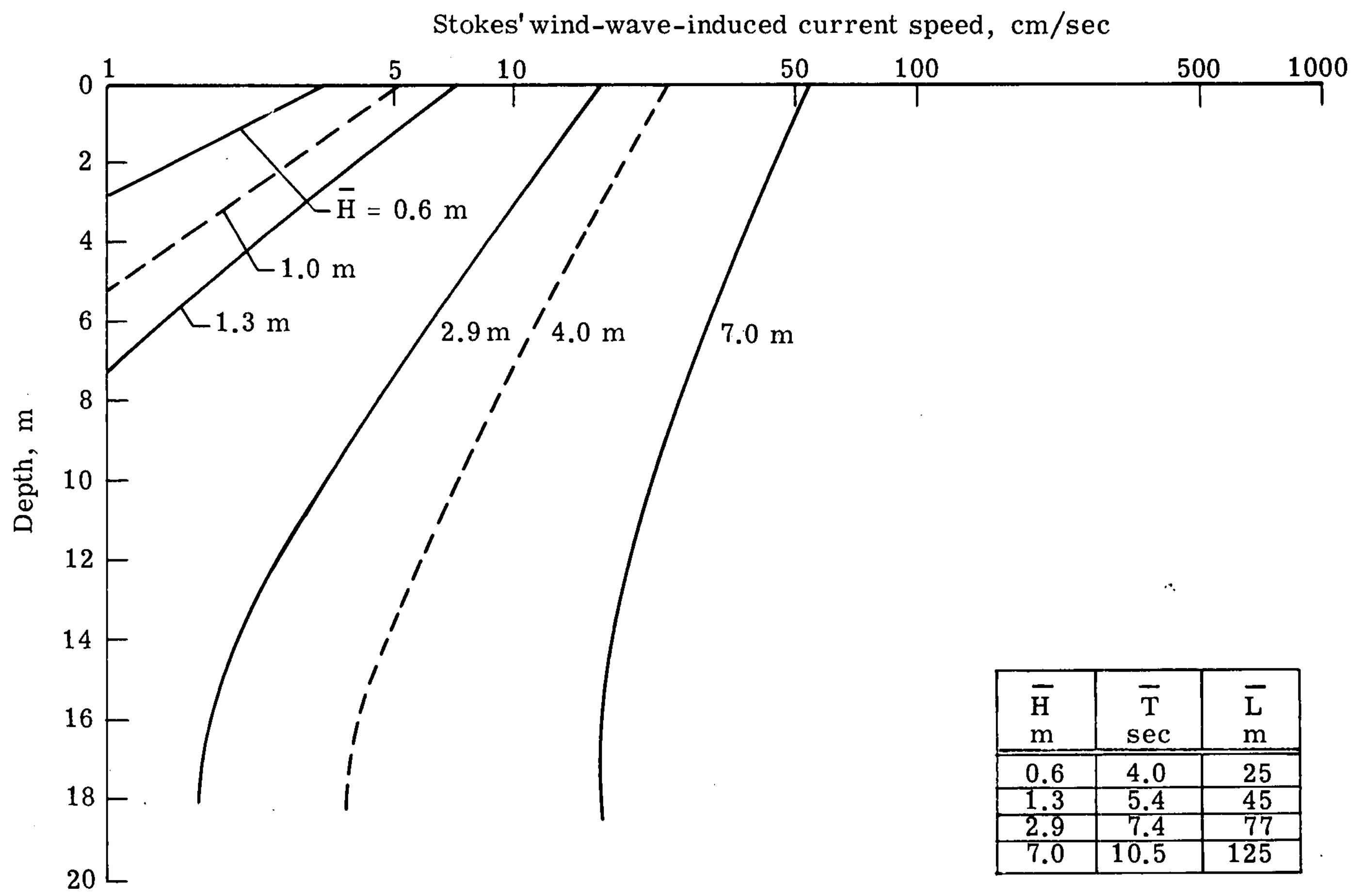

$\bar{H}$, m	$\bar{T}$, sec	$\bar{L}$, m
0.6	4.0	25
1.3	5.4	45
2.9	7.4	77
7.0	10.5	125

(b) Water depth, 36.6 meters.

Figure 8.- Concluded.

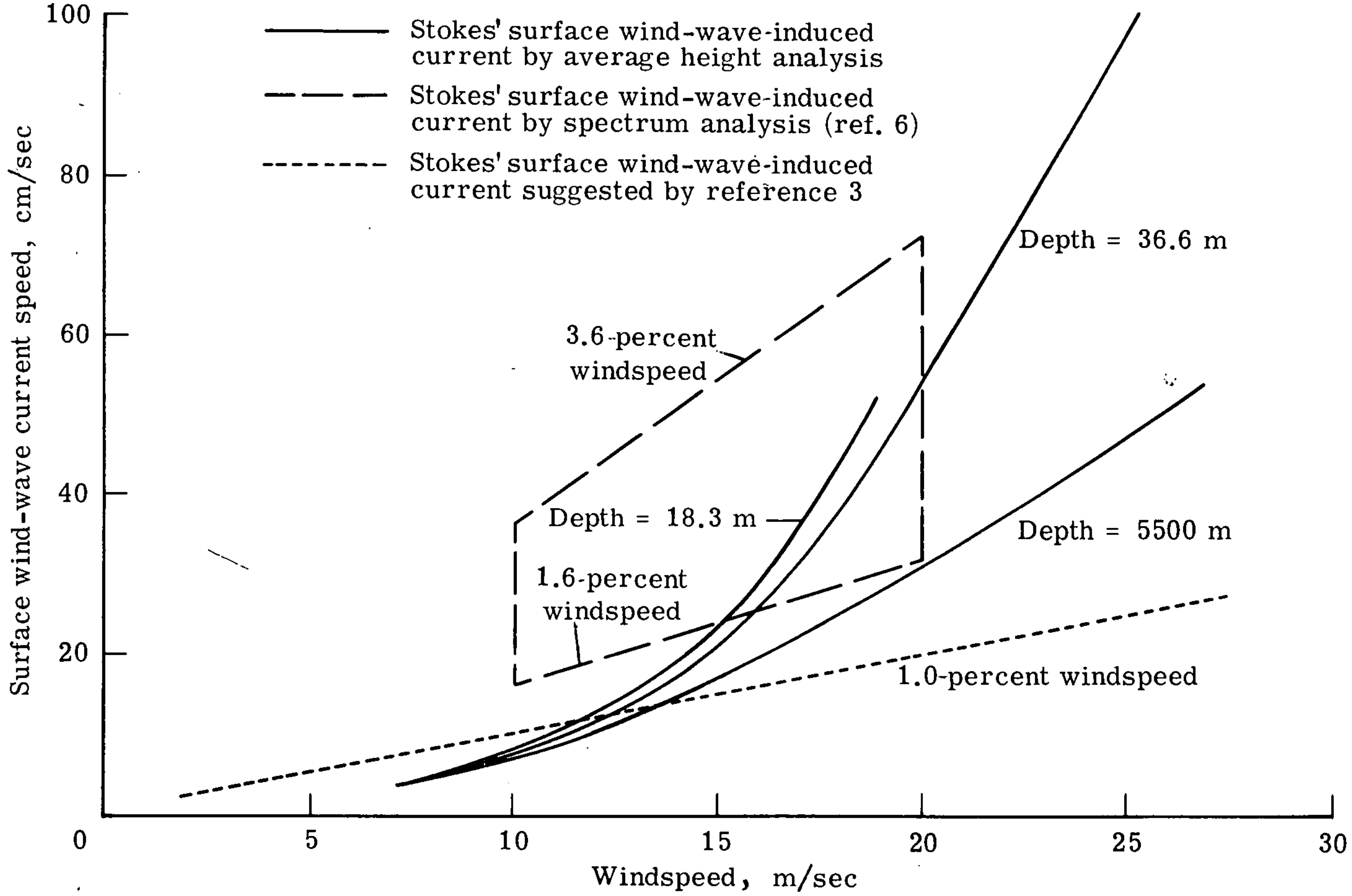

Figure 9.- Surface wind-wave currents versus windspeed.

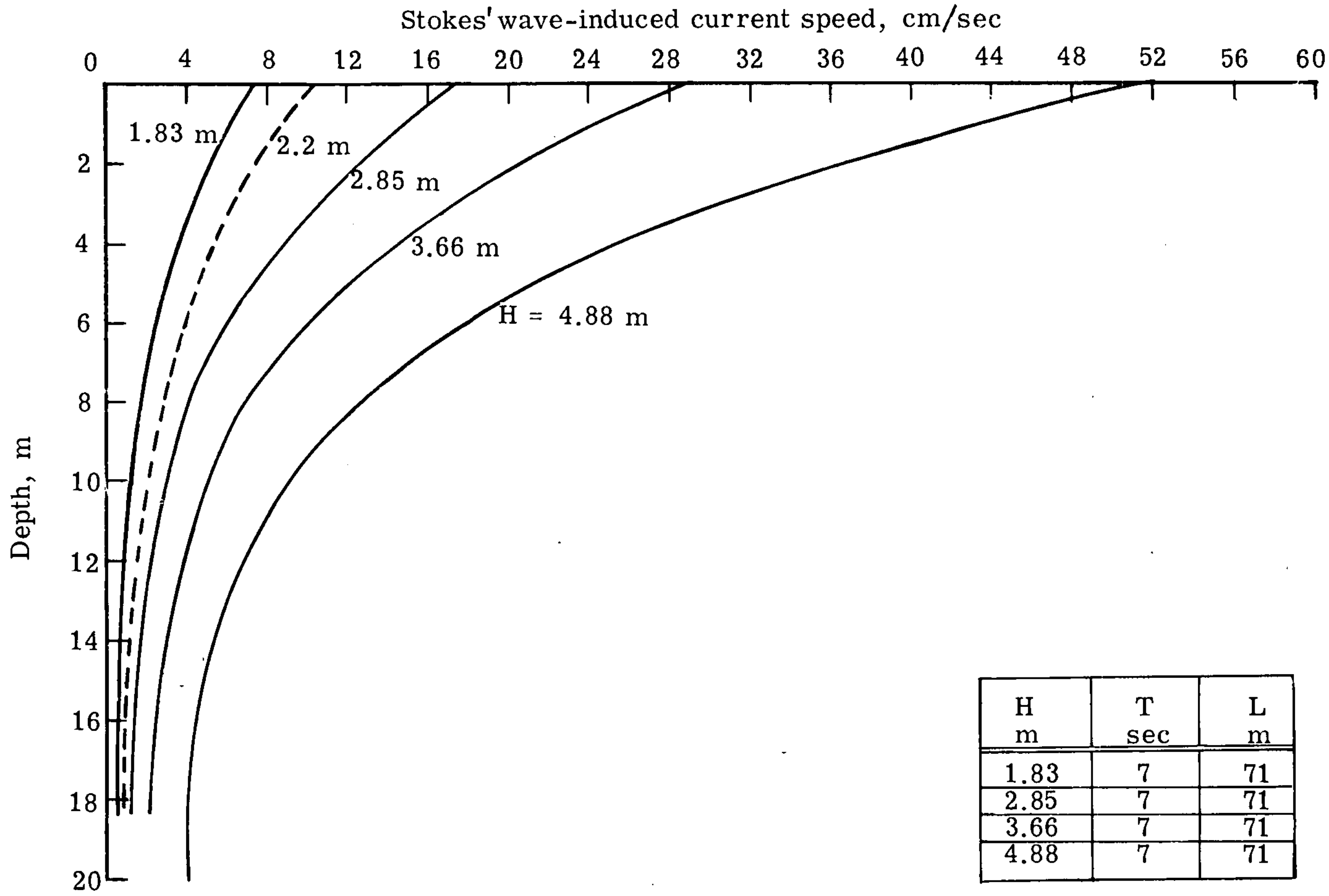

H m	T sec	L m
1.83	7	71
2.85	7	71
3.66	7	71
4.88	7	71

(a) Water depth, 18.3 meters; swell period, 7.0 seconds.

Figure 10.- Stokes' ocean-swell current-speed profiles. (Dashed lines are additional wave-induced current calculations.)

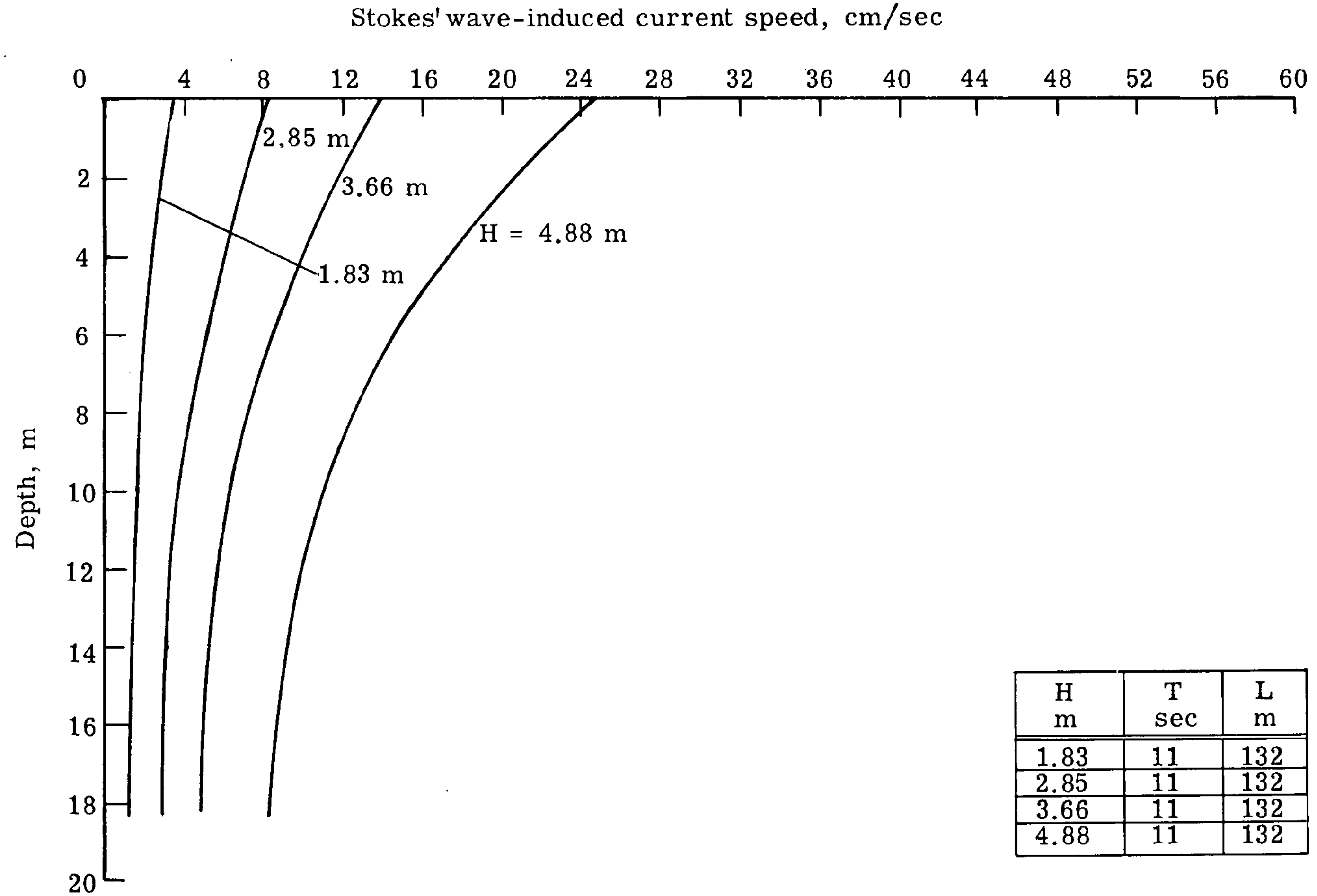

H m	T sec	L m
1.83	11	132
2.85	11	132
3.66	11	132
4.88	11	132

(b) Water depth, 18.3 meters; swell period, 11.0 seconds.

Figure 10.- Continued.

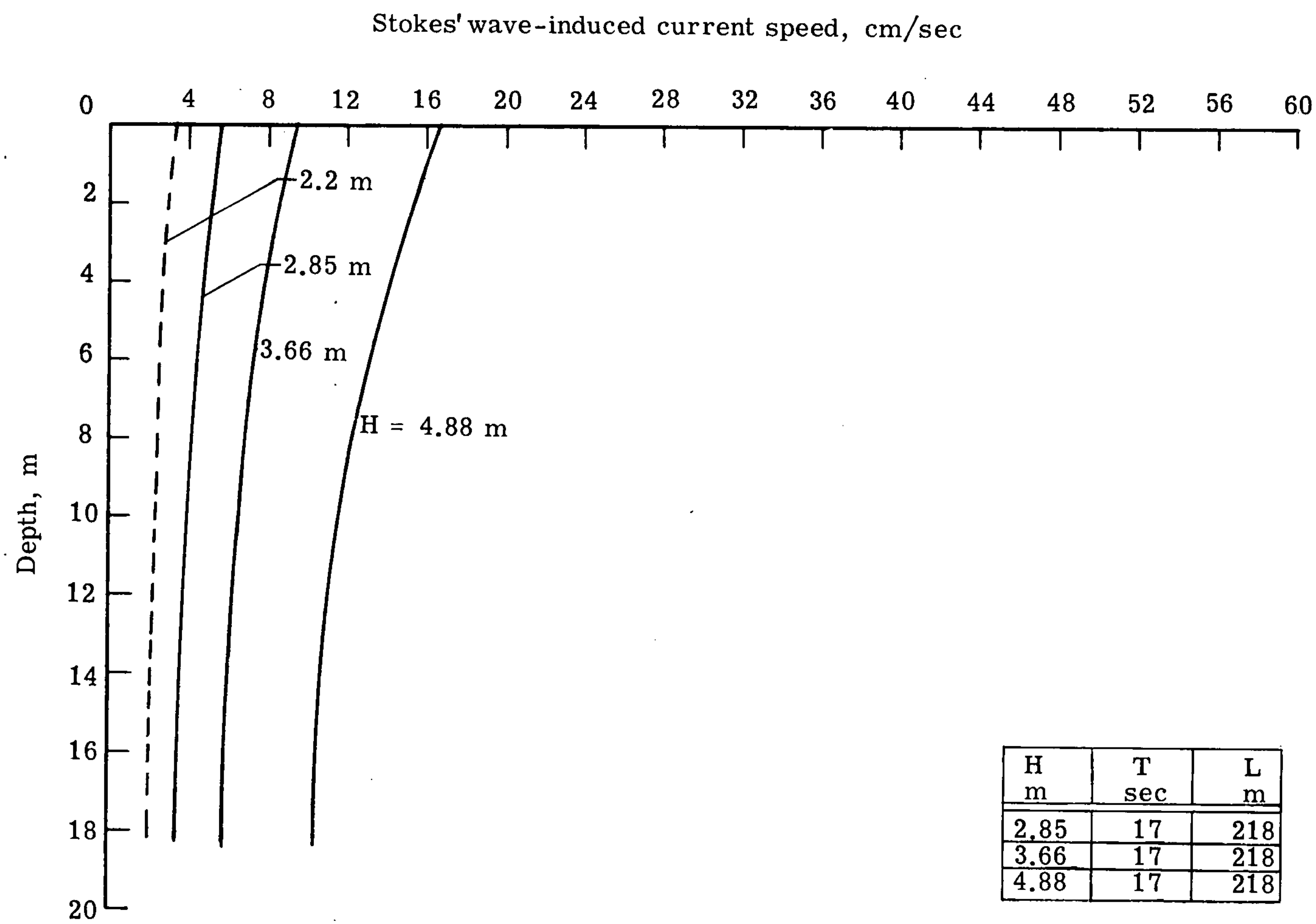

H m	T sec	L m
2.85	17	218
3.66	17	218
4.88	17	218

(c) Water depth, 18.3 meters; swell period, 17.0 seconds.

Figure 10.- Continued.

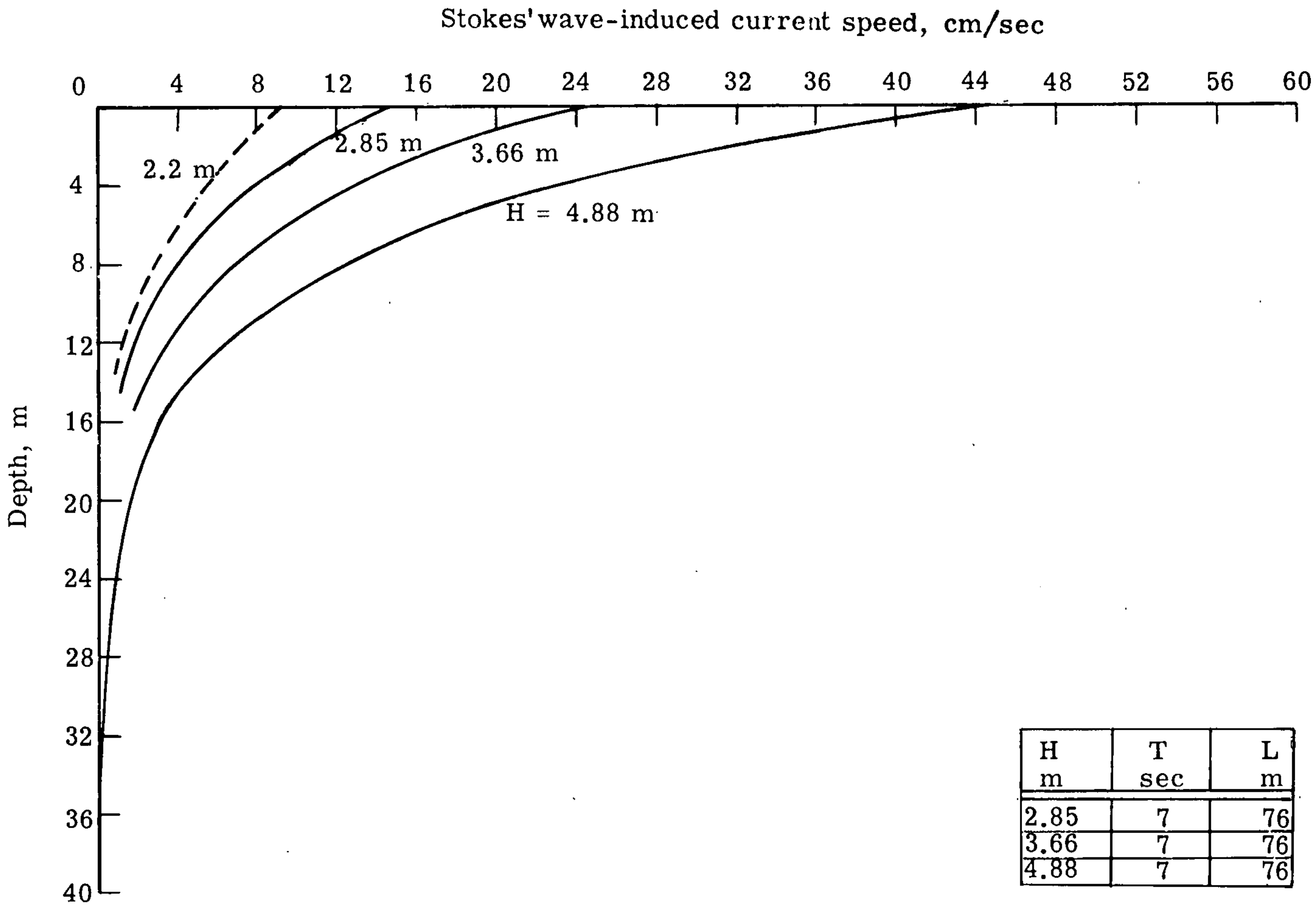

H m	T sec	L m
2.85	7	76
3.66	7	76
4.88	7	76

(d) Water depth, 36.6 meters; swell period, 7.0 seconds.

Figure 10.- Continued.

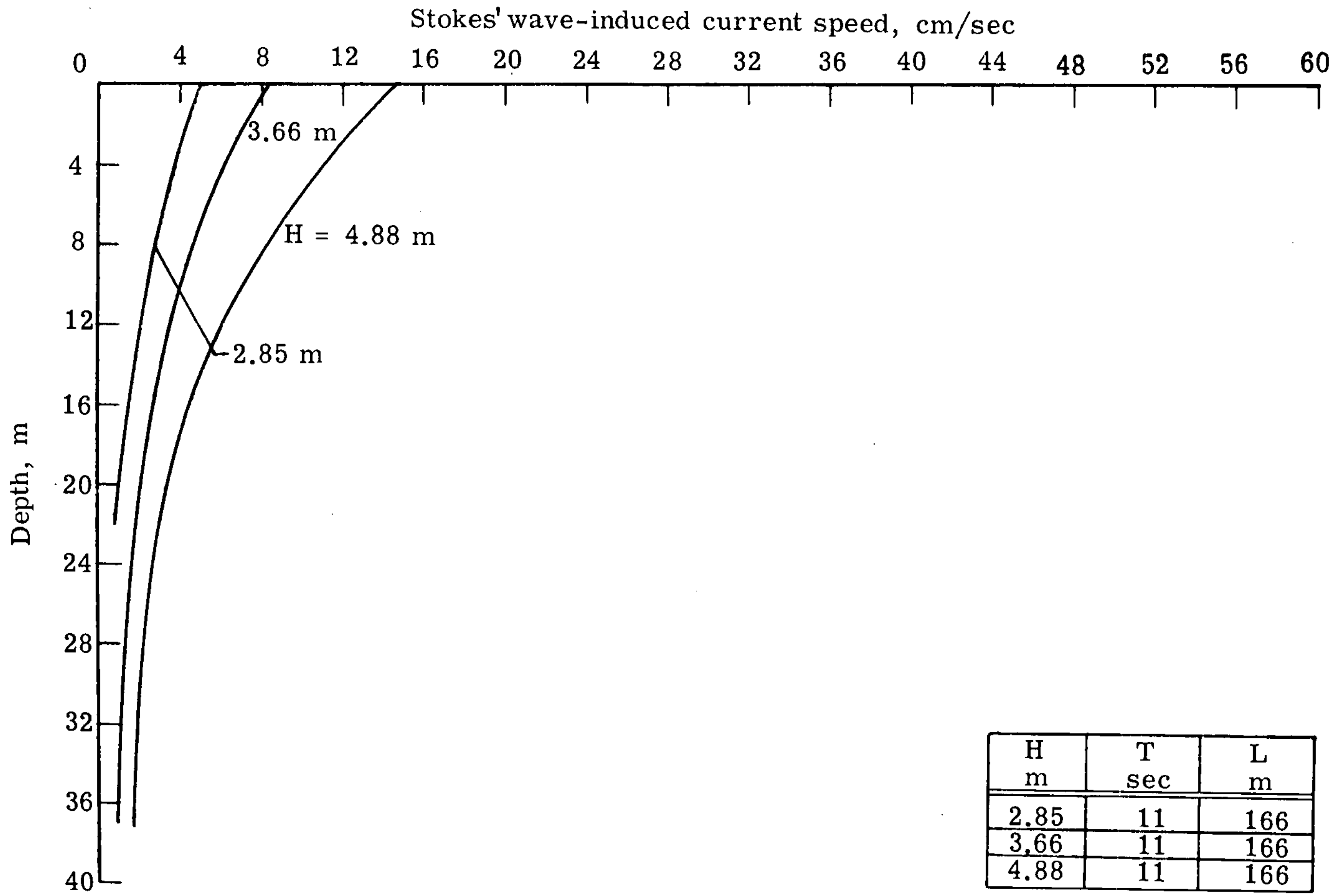

H m	T sec	L m
2.85	11	166
3.66	11	166
4.88	11	166

(e) Water depth, 36.6 meters; swell period, 11.0 seconds.

Figure 10.- Continued.

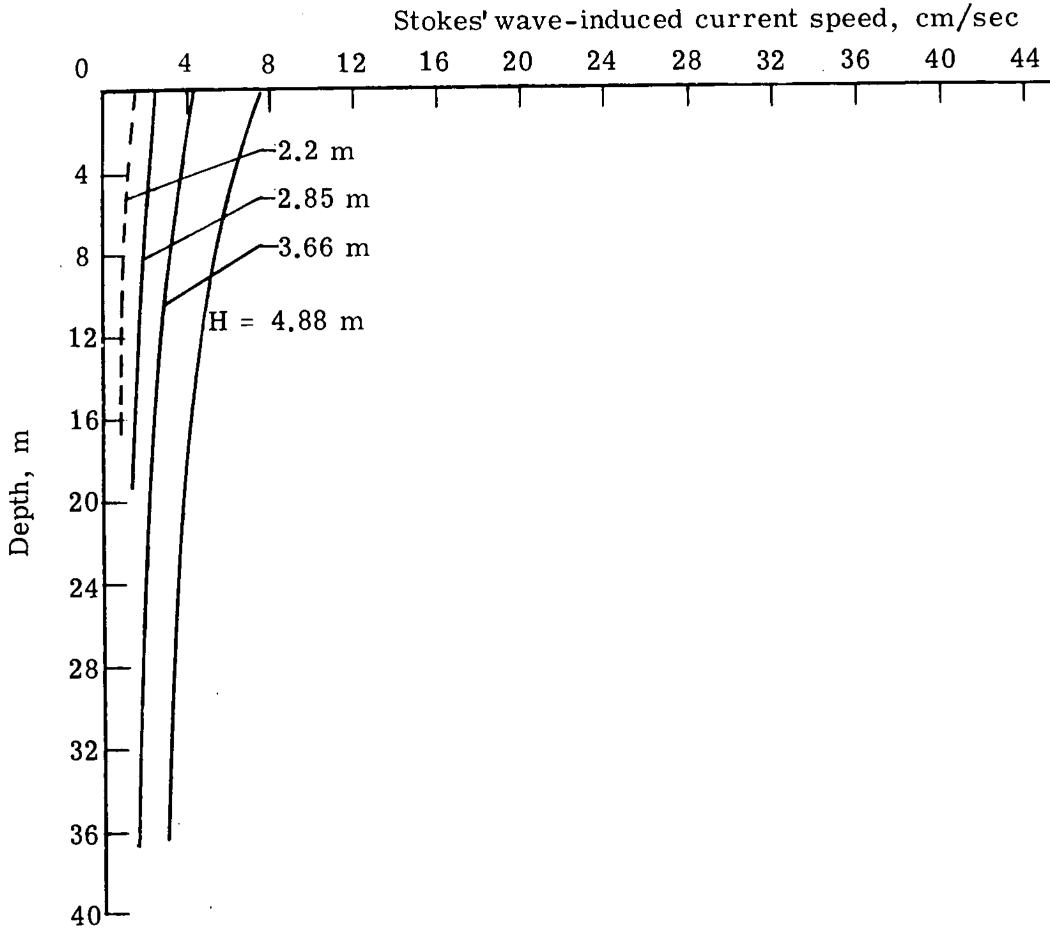

H m	T sec	L m
2.85	17	295
3.66	17	295
4.88	17	295

(f) Water depth, 36.6 meters; swell period, 17.0 seconds.

Figure 10.- Concluded.

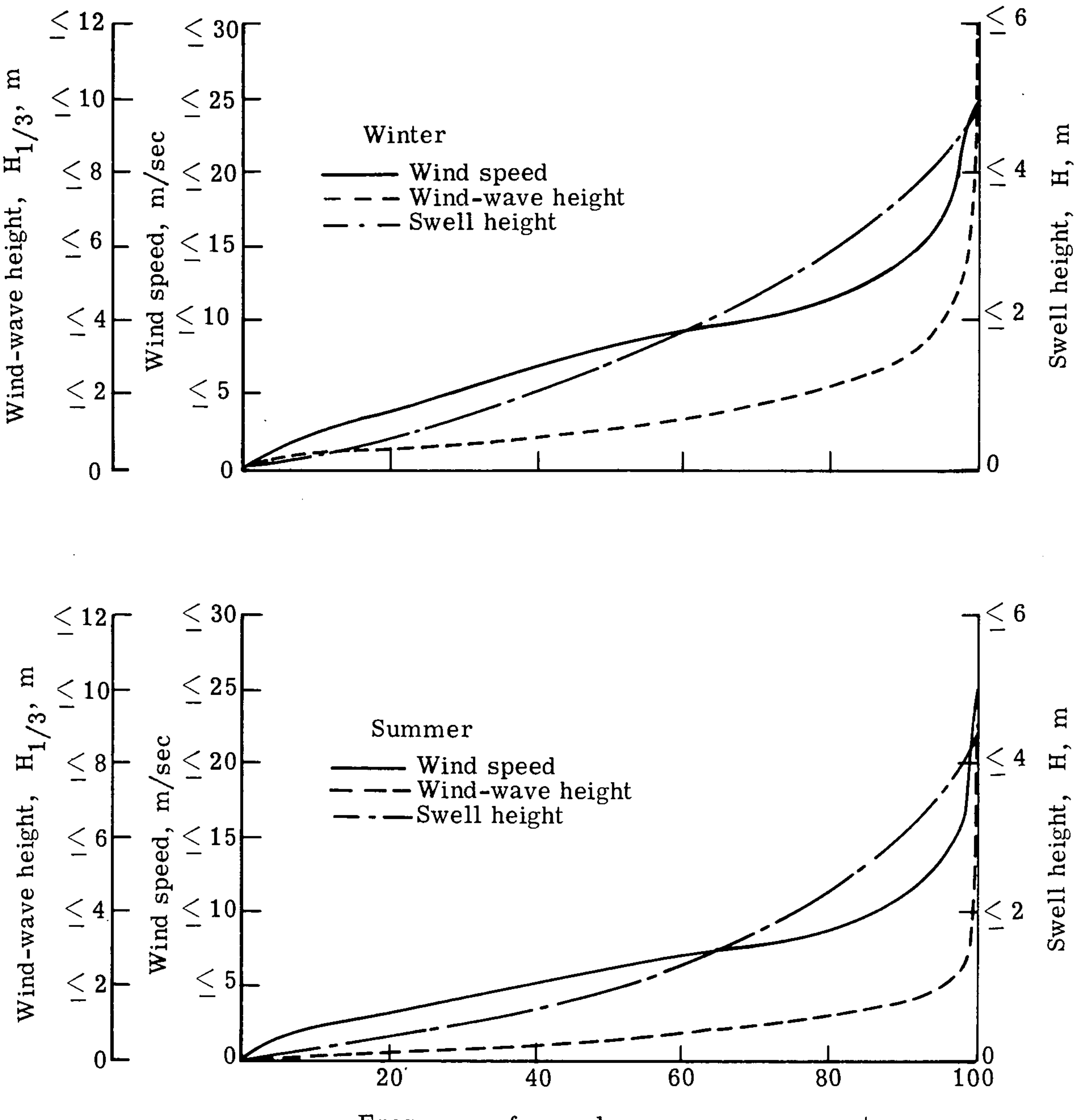

Figure 11.- Occurrence frequencies of windspeed, wind-wave height, and swell height (ref. 8).

"The aeronautical and space activities of the United States shall be conducted so as to contribute . . . to the expansion of human knowledge of phenomena in the atmosphere and space. The Administration shall provide for the widest practicable and appropriate dissemination of information concerning its activities and the results thereof."

—NATIONAL AERONAUTICS AND SPACE ACT OF 1958

NASA SCIENTIFIC AND TECHNICAL PUBLICATIONS

TECHNICAL REPORTS: Scientific and technical information considered important, complete, and a lasting contribution to existing knowledge.

TECHNICAL NOTES: Information less broad in scope but nevertheless of importance as a contribution to existing knowledge.

TECHNICAL MEMORANDUMS: Information receiving limited distribution because of preliminary data, security classification, or other reasons. Also includes conference proceedings with either limited or unlimited distribution.

CONTRACTOR REPORTS: Scientific and technical information generated under a NASA contract or grant and considered an important contribution to existing knowledge.

TECHNICAL TRANSLATIONS: Information published in a foreign language considered to merit NASA distribution in English.

SPECIAL PUBLICATIONS: Information derived from or of value to NASA activities. Publications include final reports of major projects, monographs, data compilations, handbooks, sourcebooks, and special bibliographies.

TECHNOLOGY UTILIZATION PUBLICATIONS: Information on technology used by NASA that may be of particular interest in commercial and other non-aerospace applications. Publications include Tech Briefs, Technology Utilization Reports and Technology Surveys.

Details on the availability of these publications may be obtained from:

SCIENTIFIC AND TECHNICAL INFORMATION OFFICE

NATIONAL AERONAUTICS AND SPACE ADMINISTRATION

Washington, D.C. 20546